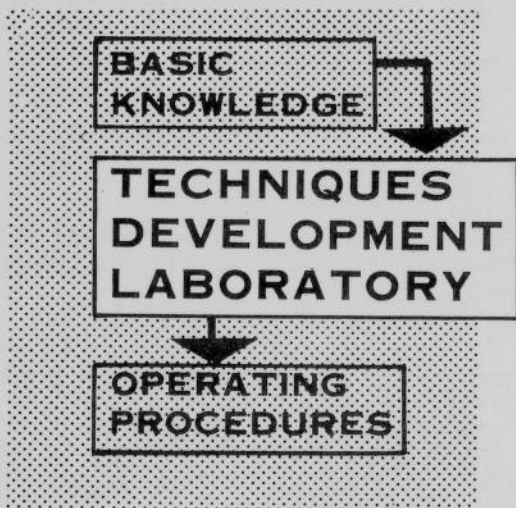


TECHNICAL NOTE 47

TECHNICAL NOTE 47-TDL-5

Hemispheric Specification of Sea Level Pressure from Numerical 700-mb. Height Forecasts



TECHNIQUES DEVELOPMENT
LABORATORY

REPORT NO. 5

WASHINGTON, D.C.

JUNE 1966

WEATHER BUREAU TECHNICAL NOTES

Techniques Development Laboratory Reports

The primary purpose of the Techniques Development Laboratory of the Systems Development Office is to translate increases in basic knowledge in meteorology and allied disciplines into improved operating techniques and procedures. To achieve this goal, TDL conducts and sponsors applied research and development aimed at the improvement of diagnostic and prognostic methods for producing weather information primarily intended to be issued directly to the public and other user groups. It carries out studies both for the general improvement of prediction methodology used in the National Meteorological Service System and for more effective utilization of weather forecasts by the ultimate user. The Laboratory makes extensive use of high speed electronic computers, special networks for measurement of meteorological phenomena, and modern prognostic techniques based on physical, dynamical, and statistical principles.

Some of the reports produced by the Techniques Development Laboratory will be reproduced in this series in order to facilitate the prompt distribution of material which may be preliminary in nature. Reports by Weather Bureau contractors working with TDL may also appear in this series. Since these Technical Notes may not be in completely polished form and are for limited reproduction and distribution, they do not constitute formal scientific publication. Therefore, reference to a paper in this series should identify it as an unpublished report.

The reports are available through the Clearinghouse for Federal Scientific and Technical Information, U. S. Department of Commerce, Sills Building, Port Royal Road, Springfield, Virginia - 22151.

- No. 1 Objective Prediction of Daily Surface Temperature by William H. Klein, Curtis W. Crockett, and Carlos R. Dunn. October 1965.
- No. 2 Hurricane Cindy Galveston Bay Tides, N. A. Pore, A. T. Angelo, and J. G. Taylor. Sept. 1965.
- No. 3 Atmospheric Effects on Re-Entry Vehicle Dispersions. Karl R. Johannessen, Dec. 1965.
- No. 4 A Synoptic Climatology of Winter Precipitation from 700-mb. Lows for the Intermountain Areas of the West. D. L. Jorgensen, W. H. Klein, and A. F. Korte. May 1966.

U.S. DEPARTMENT OF COMMERCE • John T. Connor, Secretary

ENVIRONMENTAL SCIENCE SERVICES ADMINISTRATION

Robert M. White, Administrator

Weather Bureau • George P. Cressman, Director

TECHNICAL NOTE 47-TDL-5

Hemispheric Specification of Sea Level Pressure from Numerical 700-mb. Height Forecasts

William H. Klein
Techniques Development Laboratory, Washington, D.C.

Billy M. Lewis
National Hurricane Research Laboratory, Miami, Fla.

TECHNIQUES DEVELOPMENT
LABORATORY

REPORT NO.5

WASHINGTON, D.C.
JUNE 1966



CONTENTS

ABSTRACT	1
1. INTRODUCTION	1
2. BASIC DATA AND PROCEDURE	2
3. CLIMATOLOGICAL RESULTS	6
4. SPECIFICATION EQUATIONS	10
5. OPERATIONAL ASPECTS	21
6. VERIFICATION AND CONCLUSION	23
ACKNOWLEDGMENT	30
REFERENCES	30

HEMISPHERIC SPECIFICATION OF SEA LEVEL PRESSURE
FROM NUMERICAL 700-MB. HEIGHT FORECASTS

WILLIAM H. KLEIN

Techniques Development Laboratory, Washington, D. C.

and

BILLY M. LEWIS

National Hurricane Research Laboratory, Miami, Fla.

ABSTRACT

An objective method of translating a map of 700-mb. height into its accompanying chart of sea level pressure is derived from 17 years of daily data at 469 grid points covering the Northern Hemisphere during every other month of the year. The method involves application of the screening technique to derive multiple regression equations which automatically incorporate a prediction of thickness implied by the 700-mb. circulation. On the average, the specification equations explain almost 70 percent of the pressure variance by means of approximately three heights and have a standard error of estimate of about 4mb. The variation of these and other properties of the equations with geography, latitude, and month is illustrated and discussed.

The equations have been programmed with the aid of spatial harmonic analysis, so that automatic, curve-followed, sea level pressure maps can be produced in a few minutes. The program has been applied to 36-hr. baroclinic and 72-hr. barotropic prognostic heights routinely prepared in the National Meteorological Center. The resulting objective forecasts of the hemispheric sea level pressure field are illustrated and compared with predictions produced by other methods.

Valuable climatological material is also presented, particularly hemispheric monthly maps of the standard deviation of daily 700-mb. height and sea level pressure and the correlation between these variables.

1. INTRODUCTION

Statistical prediction of tomorrow's sea level pressure from today's pressure at a network of surrounding cities of means of ordinary multiple regression was attempted during World War II independently by both Schumann [19] and Wadsworth [26]. The number of possible predictors was reduced by Miller and Malone [14], who used Tschebysheff orthogonal polynomials in 1956 to predict daily sea level pressure at 91 grid points in North America. In order to derive a completely uncorrelated set of predictors, Lorenz [10] replaced the Tschebysheff polynomials by a set of empirical functions which would be mutually orthogonal in time as well as space. These so-called "empirical orthogonal functions" were used by Shorr [21] to predict sea level pressure in the United States, and the method was extended to a hemispheric scale by White et al. in 1958 [27].

An alternate method for conserving degrees of freedom is the screening procedure, a stepwise method of multiple regression introduced to meteorology by Bryan (unpublished) and Miller [13]. Screening was applied extensively to derive prediction equations for sea level pressure at a few cities by Miller [13], for hurricane motion by Veigas et al. [24], for east coast cyclones by Veigas and Ostby [25], for sea level pressure change by Lund [11], for anticyclone motion by Martin et al. [12], and for typhoon motion by Arakawa [1].

Although results of the above studies were promising, few were applied in operational forecasting, largely because of the success which has been achieved in predicting the circulation pattern by dynamical methods. However, experience with numerical weather predictions during the past decade has demonstrated that both baroclinic and barotropic models give better results in the mid troposphere than at sea level [3]. Although a numerical model for 1000-mb. prognosis developed by Reed [16] has been found quite helpful as a forecast aid, prognostic charts transmitted over facsimile by the National Meteorological Center (NMC) in Suitland, Md., are still prepared objectively for upper levels but subjectively for the surface.

The purpose of the present study was to develop a completely objective method of translating an upper-level height forecast into its accompanying chart of sea level pressure. This has been accomplished by applying the screening technique to a historical file of observed maps and then applying the resultant regression equations to numerical prognostic heights. A similar combination of statistical and dynamical techniques was used for objective prediction of surface temperature [8], clouds and precipitation [7], and sea level pressure [17].

In a recent paper [5], multiple regression equations were derived for sea level pressure at 70 points in and near North America by applying the screening technique to 10 years of 5-day mean 700-mb. height, with all data expressed as departures from normal at a rather coarse grid of points. On the basis of extensive tests with this method, the following conclusions were drawn:

1. There is no appreciable lag between sea level pressure and 700-mb. height, so that specification from a concurrent chart offers more promise than prediction from an earlier one.
2. There is no appreciable difference in the accuracy, nature, or behavior of equations derived from daily or 5-day mean data.
3. No appreciable improvement is obtainable by the inclusion of earlier heights or pressures as predictors.
4. In general, equations with a small number of terms hold up better on independent data than those with a large number.

2. BASIC DATA AND PROCEDURE

In view of these conclusions, a project was conducted to derive multiple regression equations for specifying daily sea level pressure from simultaneous

daily 700-mb. height over the entire Northern Hemisphere. This was done separately for every other month of the year by applying the screening program to each day of 1200 GMT grid point data¹ in the historical file of the Extended Forecast Division of the National Meteorological Center. Here synoptic maps of 700-mb. height and sea level pressure covering most of the Northern Hemisphere have been carefully analyzed twice daily, and heights and pressures at standard intersections of latitude and longitude have been routinely interpolated from these analyses and entered on punched cards. Since the 700-mb. maps were analyzed in part by upward extrapolation from sea level, analyses at the two levels are not completely independent, and this may color the results of this investigation, particularly in regions of sparse data.

Two separate derivations were made, one for the even grid of points, shown by dots in figure 1, for every 10° of latitude from 20°N. to 90°N., and the other for the odd grid, shown by boxes in figure 1, for every 10° of latitude from 25°N. to 75°N. The period of record began on January 1, 1947, in most of the Western Hemisphere, on January 1, 1948, in most of the Arctic and northern Siberia, and on January 1, 1951, at low latitudes of the Eastern Hemisphere. The exact areas and dates used are delineated in figure 1. No derivation was made in the Tropics because of inadequate data. Since the input data ended on December 31, 1963, there were 17 years of data in the Western Hemisphere, 16 years in the Arctic, and 13 years in the Eastern Hemisphere.

Since the particular screening program used for this study could accommodate a maximum of only 50 dependent and 150 independent variables, since 469 grid points in the Northern Hemisphere were considered, and since different periods of record were available in different areas (fig. 1), a total of 15 screening runs was made for each month. Table 1 shows the area and number of variables in each run. There were three basic groups corresponding to the three areas of figure 1. The Western Hemisphere was covered by three runs for the even and two runs for the odd grid, the Arctic area by three runs for the even and three runs for the odd grid, and the Eastern Hemisphere by two runs for the even and two runs for the odd grid. The North Pole was included only once - as the last variable in run number 6. Since the runs covered partly overlapping areas, some points had more than one derivation, and in these cases preference was given to the run based on the longest period of record.

It would have been desirable to express all pressures and heights as departures from a daily normal, but this would have required considerable extra work. Therefore, all pressures and heights were taken as absolute values, and the effect of seasonal trend was removed by including the day of the month as the last independent variable in each screening run. This is a simplified version of a scheme used successfully by Russo, Enger, and Sorenson [18].

¹Prior to June 1, 1957, the sea level maps were based on 1230 GMT data, and the upper-air maps on 1500 GMT data. The small errors introduced by these time differences have been neglected in this study.

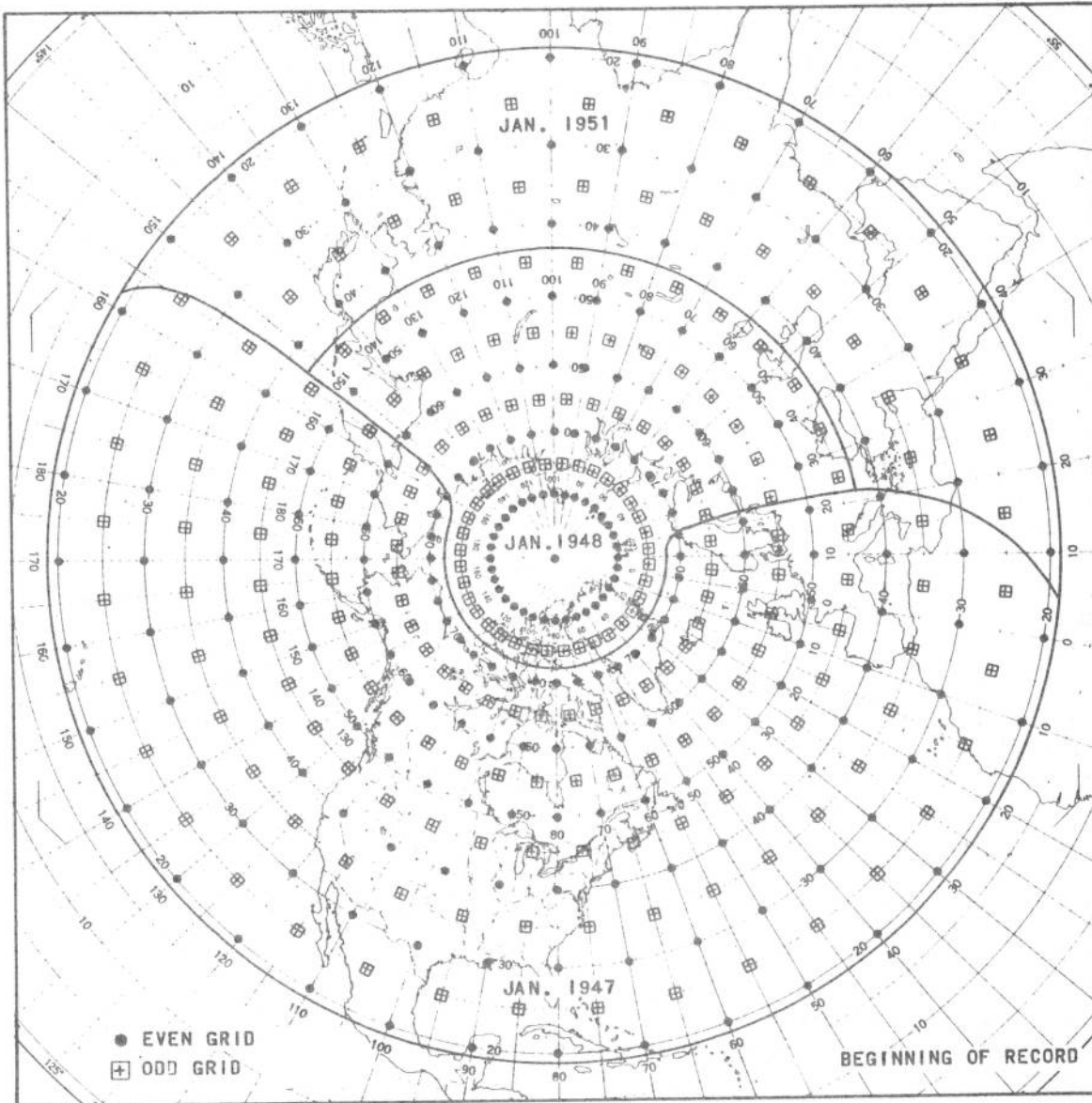


Figure 1. - Diamond grid of points for which data were processed and first month used in derivation. Equations were derived for 253 points in the even grid (dots) and 216 points in the odd grid (squares).

Table 1. - Areas covered and number of variables used in different screening runs to derive equations for specifying sea-level pressure as a function of 700-mb. height on a hemispheric basis.

Run	Area	Grid	Lat(°N)	Longitudes			
				Pressure	No.	Height	No.
1	western	even	20-70	340-050	48	340-200	138
2	western	even	20-70	060-130	48	340-200	138
3	western	even	20-70	140-200	48	340-200	138
4	western	odd	25-65	355-085	50	345-205	115
5	western	odd	25-65	095-185	50	345-205	115
6	arctic	even	50-80	000-110	48	000-350	144
7	arctic	even	50-80	120-230	48	000-350	144
8	arctic	even	50-80	240-350	48	000-350	144
9	arctic	odd	45-75	005-115	48	005-355	144
10	arctic	odd	45-75	125-235	48	005-355	144
11	arctic	odd	45-75	245-355	48	005-355	144
12	eastern	even	20-60	170-260	50	170-000	100
13	eastern	even	20-60	270-350	45	170-000	100
14	eastern	odd	25-65	175-265	50	175-005	100
15	eastern	odd	25-65	275-345	40	175-005	100

3. CLIMATOLOGICAL RESULTS

As a by-product of this investigation, considerable data of climatological interest were obtained. One example is the geographical and monthly distribution of the standard deviation of daily 700-mb. height and sea level pressure. The results are presented in map form in figures 2 and 3. Similar charts were published earlier for sea level pressure by Klein [6] and by Schumann and Van Rooy [20], and for 700-mb. height by Klein [6], Friedman [4], and Ratner [15]. However, previous data samples were considerably more restricted in size, area, and period of record than the present one.

The patterns of the charts shown here are basically similar to those published previously. In all cases the principal variation is in the meridional direction, with sharply decreasing values from about 60°N . southward. There is also considerable zonal variation, however, with smaller values over North America and Asia and larger values over oceanic areas. The relative minimum over North America is more pronounced at 700 mb. than at sea level; and east of the continental divide, a relative minimum at 700 mb. is superimposed on a relative maximum at sea level.

In all months centers of maximum appear at both sea level and 700 mb. in the vicinity of the semi-permanent Icelandic and Aleutian Lows. Additional maxima are found along the northern border of the Soviet Union or in the Arctic Ocean on most of the charts. Secondary minima frequently appear in parts of Canada and Greenland. The effects of tropical cyclones are reflected in weak centers or ridges of maximum during the summer months off the coasts of Formosa and Mexico. Otherwise there is generally little difference in the patterns between different months and between sea level pressure and 700-mb. heights. However, the magnitudes are roughly twice as great in winter as in summer.

The standard deviations shown in figures 2 and 3 were averaged by latitude with results given in table 2. In nearly all cases values increase rapidly from minima at 20°N . to maxima at 60° or 65°N ., with only slight change from there poleward. Between 65° and 80°N . variability decreases with increasing latitude during January and November, increases in March and July, and fluctuates irregularly during May and September. For the year as a whole, maximum values occur at 65°N . at both sea level and 700 mb.

Another statistic of climatological interest is the simple linear correlation coefficient between simultaneous values of sea level pressure and 700-mb. height directly overhead. This local correlation is illustrated in map form in figure 4 and in tabular form, averaged around latitude circles, in table 2. The latitudinal variation is quite similar from month to month; with positive values at all latitudes and minima at 20°N ., maxima at 80°N ., and secondary maxima at 60°N . during March, May, July, and November.

The geographical distribution of the local correlation coefficient also exhibits little seasonal variation. It exceeds 0.8 in most of the Atlantic, Pacific, and Arctic throughout the year, with maximum values greater than 0.95 off the coast of Iceland during all months except July and over the Aleutians in January and November. High correlations over maritime areas

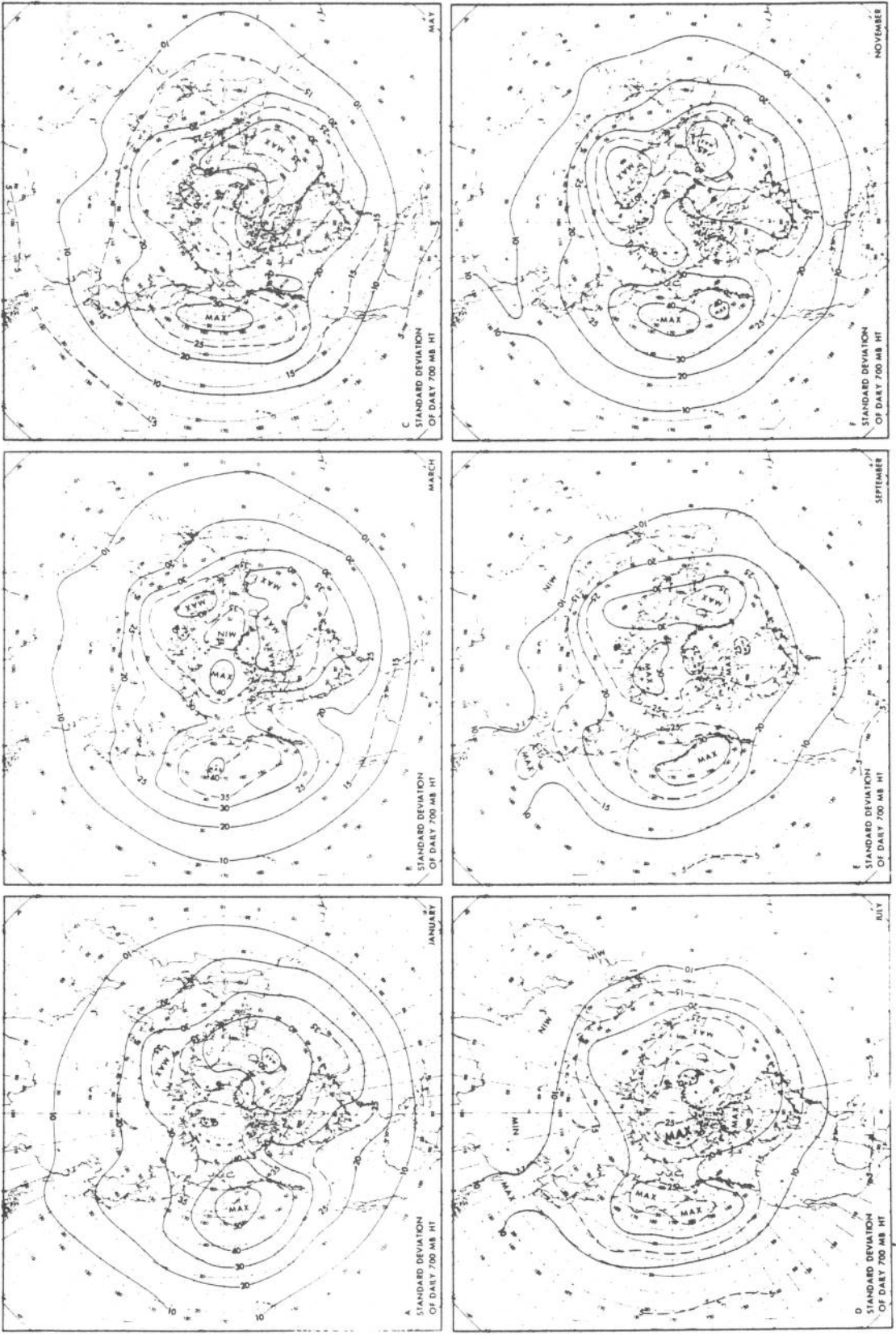


Figure 2. - Standard deviation of daily 700-mb. height for the months shown. Isopleths are in tens of feet, with centers labeled as maximum or minimum.

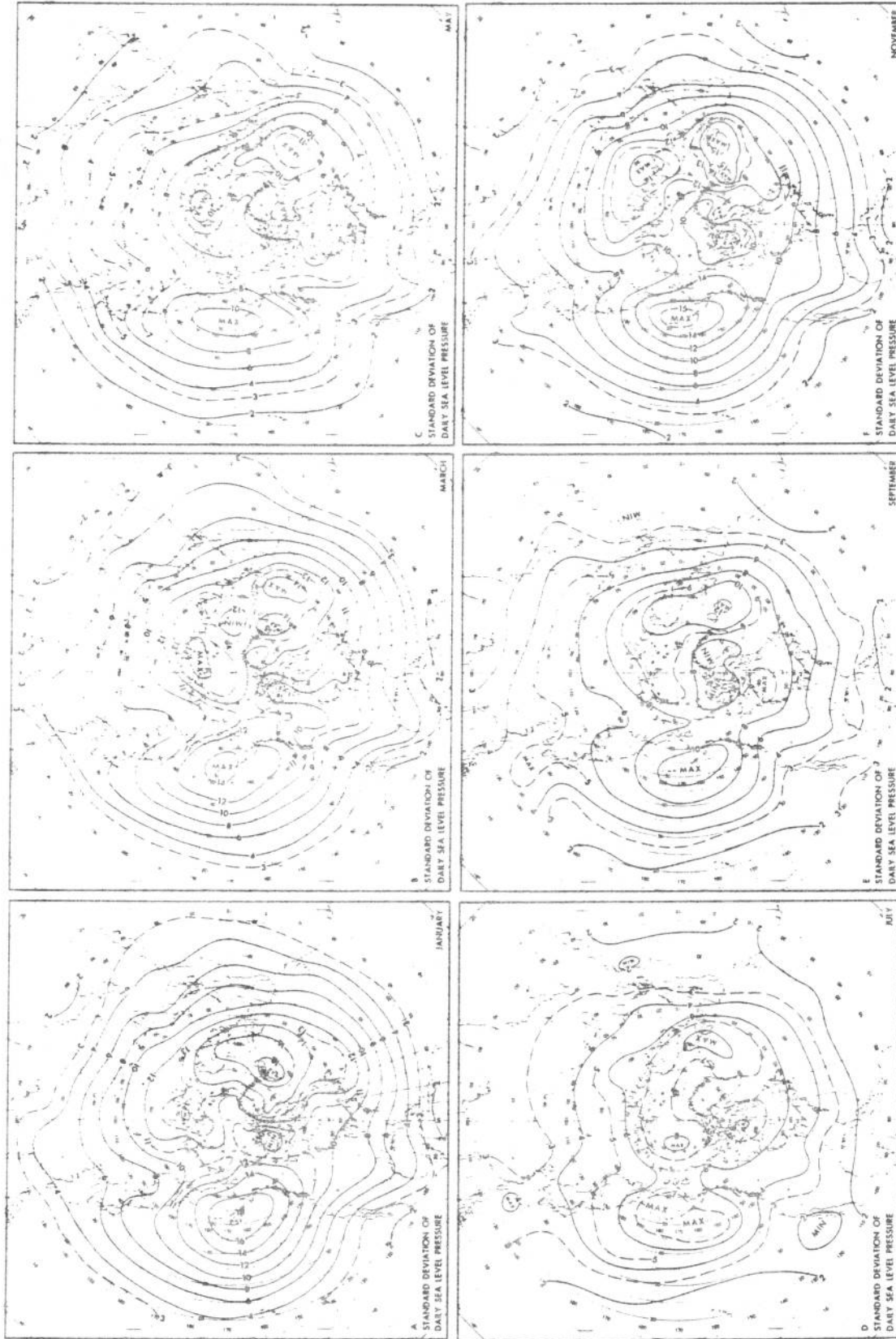


Figure 3. - Standard deviation of daily sea level pressure for the months shown. Isopleths are in millibars, with centers labeled as maximum or minimum.

Table 2. - Northern Hemisphere averages, by latitude and month, of the standard deviation of 700-mb. height (σ_7), the standard deviation of sea level pressure (σ_p), the simple correlation (r) between local pressure and height, the multiple correlation (R) between pressure and the variables used in the specification equations, the percent of pressure variance explained by these equations (EV), the standard error of estimate (σ_e) of these equations, the number of variables in these equations, the percent of equations with local height as a predictor, and the percent of equations with day of the month as a predictor.

Lat. (°N.)	σ_7 (ft.)	σ_p (mb.)	r	R	EV (%)	σ_e (ft.)	No. Var.	%Local	%Day	Lat. (°N.)	σ_7 (ft.)	σ_p (mb.)	r	R	EV (%)	σ_e (ft.)	No. Var.	%Local	%Day
(A) JANUARY:										(B) SEPTEMBER:									
20	89	2.9	.57	.69	50	2.0	2.9	78	17	20	75	2.4	.61	.69	49	1.7	2.8	97	42
25	126	4.1	.62	.75	57	2.5	2.8	61	11	25	86	2.3	.61	.73	55	1.8	3.3	99	47
30	175	5.6	.66	.79	64	3.1	3.1	56	3	30	101	3.3	.64	.78	61	2.0	3.5	89	61
35	223	7.5	.72	.82	68	3.8	2.9	83	3	35	128	4.3	.65	.80	65	2.5	3.8	86	75
40	262	9.2	.74	.84	71	4.4	3.3	86	0	40	167	5.5	.63	.81	66	3.1	3.9	86	72
45	296	10.6	.72	.83	69	5.3	2.9	81	3	45	202	6.5	.65	.82	68	3.6	3.5	78	69
50	330	11.8	.75	.84	72	5.6	2.9	92	6	50	240	7.6	.72	.85	73	3.8	3.3	81	69
55	364	12.8	.78	.86	75	5.9	2.7	81	11	55	264	8.5	.78	.87	76	4.0	3.0	92	69
60	384	13.5	.80	.87	77	6.1	2.7	81	6	60	275	8.9	.80	.87	77	4.0	3.1	89	75
65	385	13.5	.80	.86	74	6.5	2.3	72	0	65	275	8.9	.80	.87	76	4.2	3.1	78	78
70	372	12.8	.81	.86	74	6.3	2.3	64	0	70	269	8.6	.81	.87	76	4.1	2.8	53	83
75	365	12.5	.82	.86	73	6.4	2.0	39	8	75	272	8.5	.82	.87	76	4.2	2.5	36	92
80	363	12.1	.84	.86	74	6.1	1.7	39	0	80	282	8.7	.83	.88	77	4.1	2.5	11	100
Mean	287	9.9	.74	.82	69	4.9	2.6	73	5	Mean	203	6.5	.72	.82	69	3.3	3.2	74	72
(C) MARCH:										(D) NOVEMBER:									
20	54	2.6	.52	.69	49	1.9	3.7	67	42	20	77	2.5	.57	.72	52	1.7	4.4	92	81
25	114	3.7	.56	.74	56	2.3	3.6	64	36	25	99	3.2	.56	.76	58	2.0	4.6	92	97
30	159	5.1	.63	.78	62	3.0	3.4	69	42	30	134	4.4	.59	.79	63	2.6	4.6	97	94
35	204	6.8	.68	.82	68	3.6	3.4	83	35	35	182	6.2	.64	.82	67	3.4	4.3	33	78
40	244	8.5	.70	.84	71	4.1	3.3	83	47	40	232	7.9	.67	.84	72	4.0	4.1	75	72
45	277	9.8	.72	.84	71	4.9	3.1	72	44	45	277	9.6	.69	.84	72	4.8	3.6	78	61
50	310	10.8	.76	.85	74	5.1	2.8	83	47	50	318	11.1	.76	.87	76	5.0	3.3	89	58
55	335	11.4	.79	.86	75	5.3	2.7	81	44	55	340	12.1	.80	.88	79	5.2	3.4	83	50
60	346	11.6	.79	.86	75	5.6	2.5	83	42	60	342	12.3	.81	.88	78	5.4	3.1	86	39
65	346	11.8	.77	.85	73	5.9	2.6	47	44	65	338	12.0	.79	.87	76	5.6	3.3	81	56
70	347	11.7	.78	.85	73	5.9	2.5	31	31	70	326	11.2	.79	.85	73	5.6	3.1	88	56
75	355	12.1	.82	.86	74	6.1	1.8	14	0	75	322	10.8	.80	.86	73	5.5	2.8	42	22
80	376	12.7	.87	.89	79	5.8	1.4	22	0	80	316	10.6	.81	.87	75	5.3	2.7	39	31
Mean	269	9.1	.72	.83	69	4.6	2.8	61	36	Mean	254	8.8	.71	.83	70	4.3	3.6	77	61
(E) MAY:										(F) ANNUAL MEAN:									
20	70	2.1	.50	.65	44	1.6	3.6	75	56	20	79	2.4	.55	.67	47	1.8	3.4	84	42
25	90	2.8	.53	.70	50	1.9	4.0	81	83	25	98	3.1	.57	.72	53	2.0	3.6	81	51
30	120	3.7	.59	.75	57	2.3	3.9	81	86	30	129	4.1	.62	.76	59	2.5	3.6	84	56
35	159	4.9	.63	.78	62	2.9	3.8	78	83	35	167	5.5	.66	.79	64	3.1	3.6	82	55
40	192	6.1	.68	.81	66	3.4	3.4	83	72	40	205	6.9	.68	.82	67	3.6	3.5	84	49
45	220	6.9	.66	.80	65	3.9	3.2	83	61	45	240	8.1	.69	.81	68	4.2	3.2	80	43
50	248	7.7	.72	.82	68	4.0	2.8	81	56	50	274	9.1	.75	.84	72	4.4	3.0	87	41
55	270	8.2	.76	.84	72	4.1	2.8	83	61	55	298	9.9	.79	.86	75	4.6	2.8	86	39
60	275	8.2	.78	.85	73	4.1	2.8	69	31	60	307	10.2	.80	.86	76	4.7	2.7	83	41
65	276	8.4	.76	.85	73	4.2	2.9	61	36	65	307	10.2	.79	.86	74	5.0	2.7	86	44
70	272	8.4	.75	.85	72	4.4	2.7	25	94	70	302	9.9	.79	.85	73	5.0	2.6	88	45
75	267	8.6	.77	.85	73	4.4	2.5	11	100	75	303	9.9	.81	.86	74	5.0	2.2	89	37
80	261	8.4	.78	.87	73	4.1	2.4	3	100	80	307	10.0	.83	.88	76	4.8	2.0	21	39
Mean	209	6.5	.69	.80	65	3.5	3.1	63	78	Mean	232	7.6	.72	.81	68	3.9	3.0	70	45
(G) JULY:																			
20	66	2.1	.53	.60	38	1.6	2.7	97	14										
25	72	2.2	.55	.65	43	1.6	3.2	97	31										
30	82	2.5	.57	.69	49	1.8	3.2	83	47										
35	103	3.3	.61	.72	53	2.2	3.4	81	47										
40	135	4.2	.67	.75	57	2.6	3.0	92	33										
45	170	5.0	.69	.77	61	2.9	3.1	89	22										
50	198	5.7	.76	.80	68	3.1	2.6	97	11										
55	213	6.2	.80	.84	71	3.2	2.2	94	0										
60	220	6.4	.82	.85	73	3.2	2.1	92	0										
65	223	6.4	.80	.84	71	3.3	2.1	87	0										
70	223	6.6	.78	.83	70	3.6	1.9	36	8										
75	235	7.1	.83	.86	74	3.6	1.8	31	0										
80	244	7.4	.87	.88	78	3.4	1.4	14	0										
Mean	168	5.0	.71	.78	62	2.8	2.5	75	17										

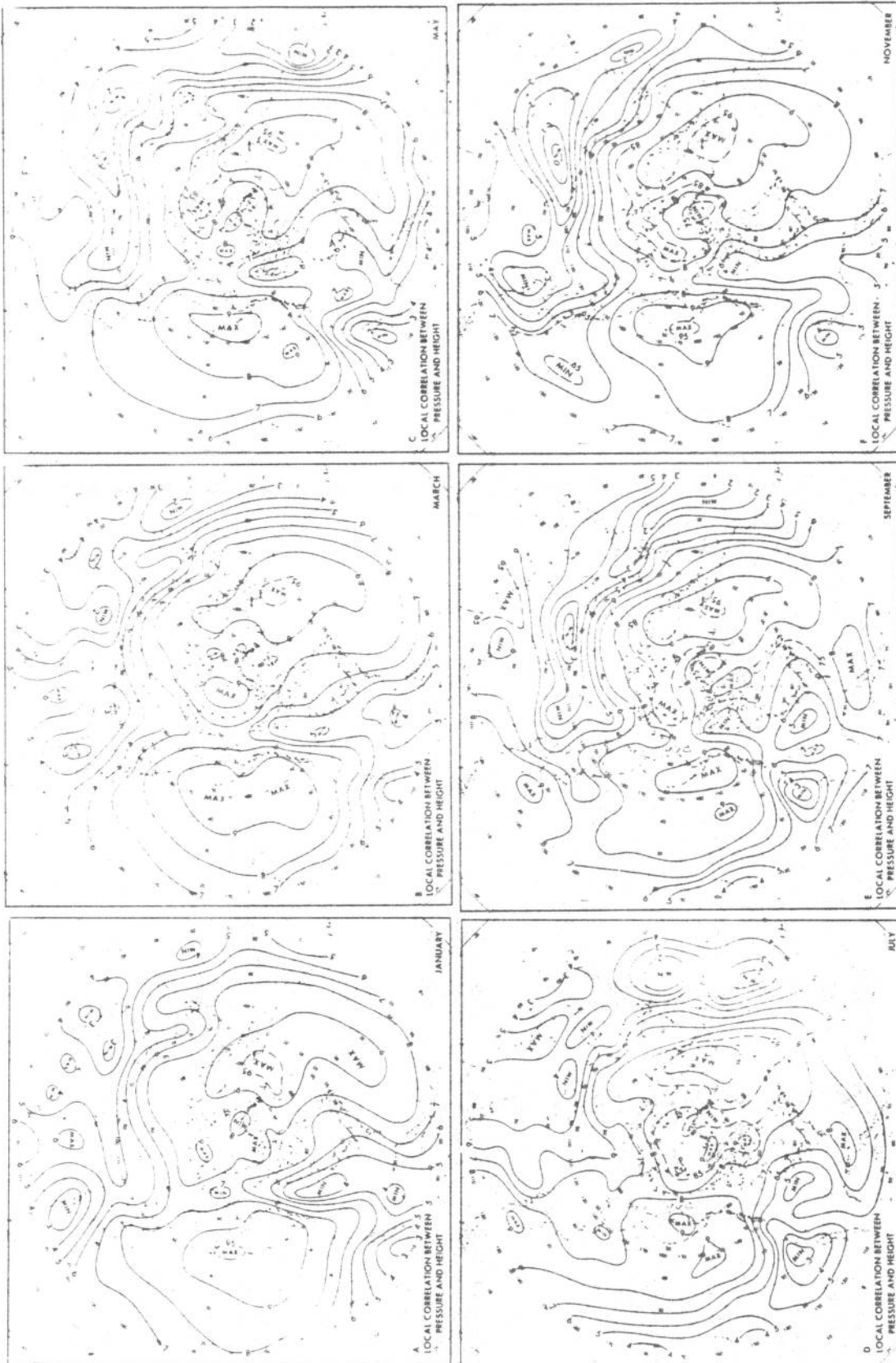


Figure 4. - Simple linear correlation coefficients for months shown between daily values of sea level pressure and concurrent 700-mb. height at the same point, with centers labeled as maximum or minimum.

reflect the prevalence of equivalent-barotropic conditions in which Lows are generally cold and Highs warm.

On the other hand, the coefficients of figure 4 are less than 0.5 in many continental areas where baroclinic conditions prevail. A well-defined axis of minimum correlation is located just east of the Rocky Mountains during all months, with values as low as 0.35 in January. This area is characterized by shallow cold Highs and warm Lows, so that local 700-mb. height is a rather poor indicator of sea level pressure. Local coefficients of less than 0.5 also occur in southern portions of North America and Asia and over North Africa, where poor data and small variability permit errors of analysis and observation to lower the correlation.

An interesting feature of figure 4 is the steady northward shift of the center of minimum correlation off the west coast of North America from 20°N. in January to 32°N. in September, when coefficients of 0.7 appear at 20°N. Somewhat similar shifts may be noted along the Asiatic coast, where maxima appear south of Japan during July and September, and in the east-central United States, where maxima appear over Florida in July and September. These are probably related to seasonal migrations of tropical cyclone activity and the belt of subtropical high pressure.

4. SPECIFICATION EQUATIONS

Figure 4 tells how well we could specify sea level pressure from just one 700-mb. height directly overhead. In order to obtain improved results, the screening regression method [13] was applied to select additional heights which contribute significantly and independently to the pressure.

Multiple regression equations resulting from this procedure are illustrated for two points for March in figure 5. The equation on the left is for the sea level pressure at 50°N., 10°W., just southwest of the British Isles. The most important single predictor of pressure at this point is the simultaneous 700-mb. height at the same point, which explains 90 percent of the pressure variance. The height which contributes the most additional information is located 10° to the east. Combination of this height with the first one explains 93 percent of the variance of pressure at the first point. Since no additional predictor is able to increase this explained variance² by even 2 percent, only these two heights were selected for the final equation.

In the equation the heights appear in the order selected. The positive sign of the first regression coefficient indicates that when heights are high at 50°N., 10°W., pressures are high there also, and conversely for low values. The negative sign of the second regression coefficient indicates that northerly flow between low heights at the second point and high heights

²In the remainder of this paper the term "explained variance" will be used to denote the percent of pressure variance explained by selected heights. It is also known as "reduction of variance" or "coefficient of determination" and is equal to the square of the multiple correlation coefficient.

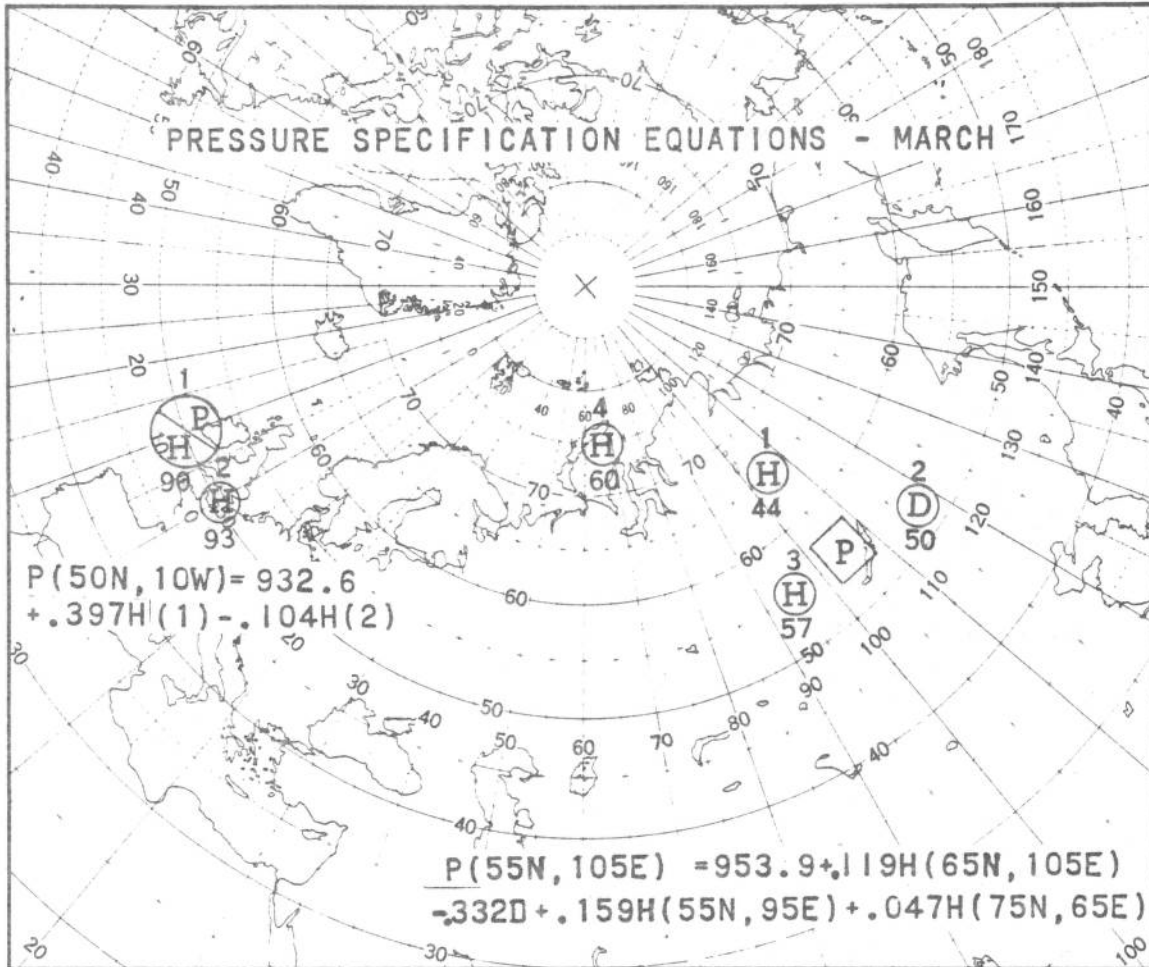


Figure 5. - Multiple regression equations used in specifying sea level pressure (p in mb.) during March. The left side is for the pressure at 50°N., 10°W. as a function of the concurrent 700-mb. height (H in tens of feet minus 700) at the same point and 10° to the east. The right side is for pressure at 55°N., 105°E. as a function of height at the points indicated and also of the day of the month (D). In both cases the location of the selected height is given by the open circle, the order of selection by the number above, and the percent of variance explained after inclusion of the given predictor by the number below.

at the first point favors high pressure, presumably through cold air advection; the converse favors low pressure under warm air advection produced by southerly flow.

This point has the closest relation between pressure and height of any point in the Northern Hemisphere during March. In all other respects,

however, its equation is typical of those derived at maritime locations of the Atlantic, Pacific, and Arctic.

A different type of equation, typical of continental areas, is illustrated on the right side of figure 5 for the sea level pressure in March at 55°N ., 105°E . just west of Lake Baikal in Siberia. Here the local 700-mb. height is not selected as one of the predictors. Instead heights 10° to the north, 10° to the west, and about 1700 mi. to the northwest are selected, with explained variance increasing gradually from 44 percent to 60 percent. The positive signs of the regression coefficients before each of these heights in the equation indicate that pressure systems near Lake Baikal normally slope northwestward from sea level to 700 mb. Another interpretation is that northeasterly flow at 700 mb. favors low thickness values and high pressure at sea level, while southwesterly flow favors high thickness values and low pressure.

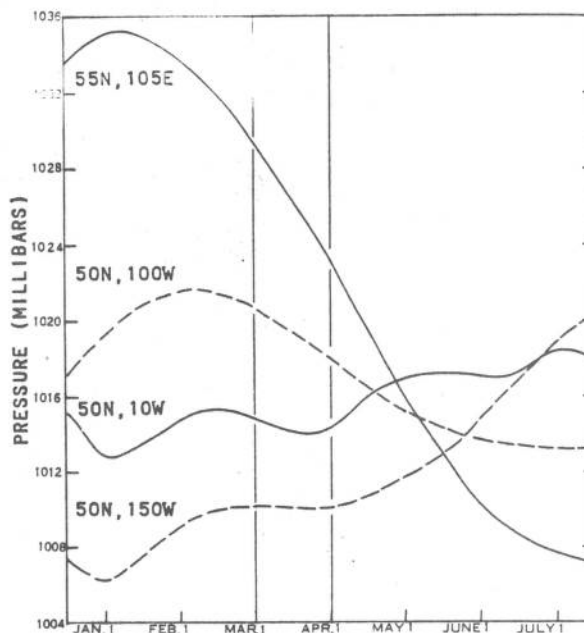


Figure 6. - Variation of normal sea level pressure from December 15 to July 15 at grid points indicated. The two vertical lines delineate the month of March. Normals were obtained from harmonic analysis of 16 years of daily data [9].

The second predictor selected in this equation is the day of the month (D), which raises the explained variance from 44 percent to 50 percent. The negative sign before the regression coefficient of this term in the final specification equation shows that sea level pressure at Lake Baikal normally decreases during the course of the month of March, as illustrated in figure 6.

Figure 6 gives the variation of normal sea level pressure from December 15 to July 15 at four different grid points and was obtained from temporal harmonic analysis (maximum of five Fourier components, Lewis [9]) of the basic synoptic data described in section 2. At 55°N ., 105°E ., near Lake Baikal, there is a marked annual cycle with an almost linear drop of pressure from March 1 to April 1. A point in central North America, at 50°N ., 100°W ., has a similar trend, but with smaller amplitude and some phase displacement. Here too, as at most points over Asia, Africa, and North America, the day of the month is selected as a predictor. On the other hand, the day is not selected over maritime locations, such as 50°N ., 10°W . in the Atlantic or 50°N ., 150°W . in the Pacific, whose curves show that the seasonal trend of pressure during March is negligible.

Figure 7 shows the percent of the pressure variance explained by the specification equations during the course of the year. Little difference in pattern is discernible from month to month, but values are somewhat lower

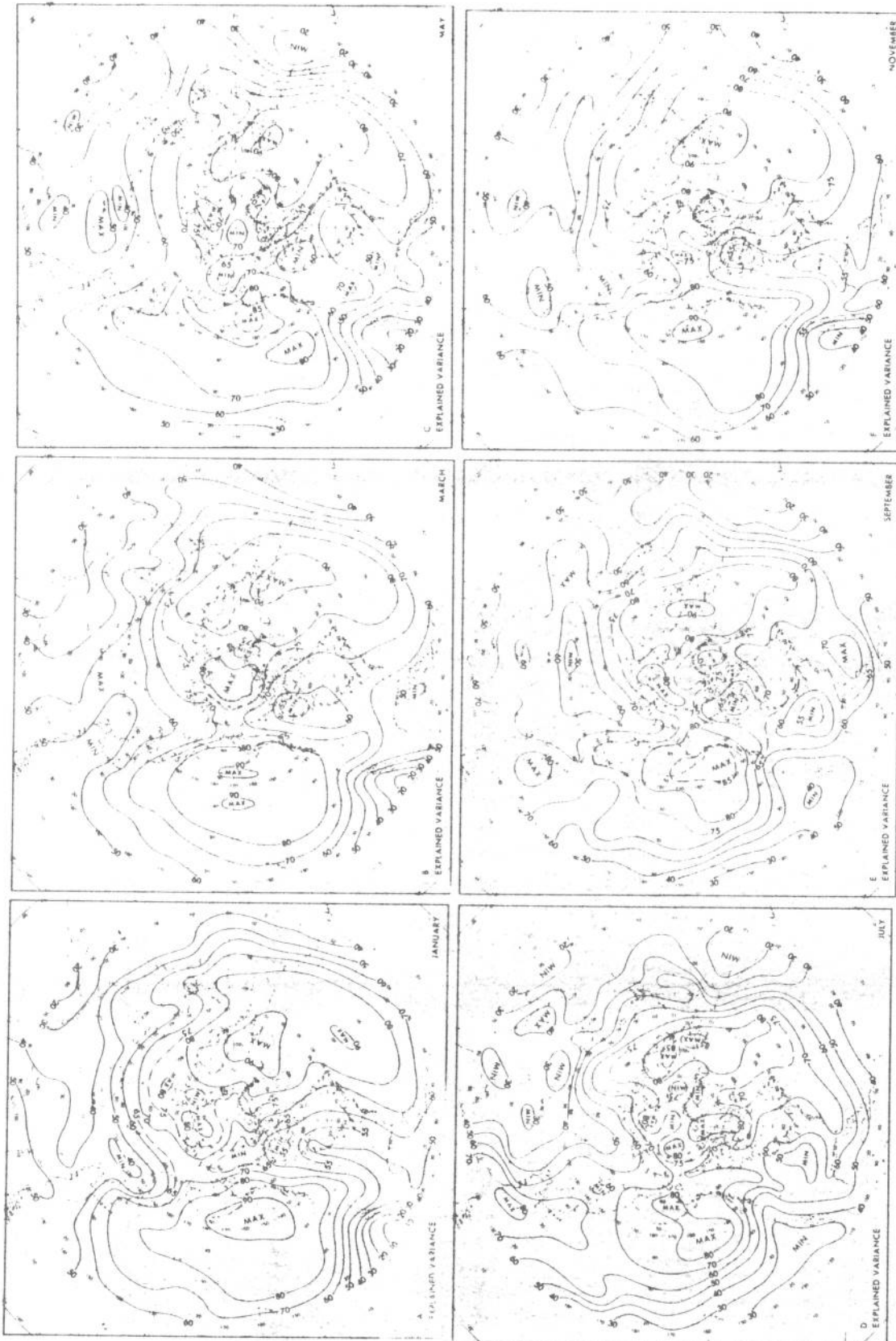


Figure 7. - Percent of variance of sea level pressure explained by specification equations of the type shown in figure 5 during months indicated, with centers labeled as maximum or minimum.

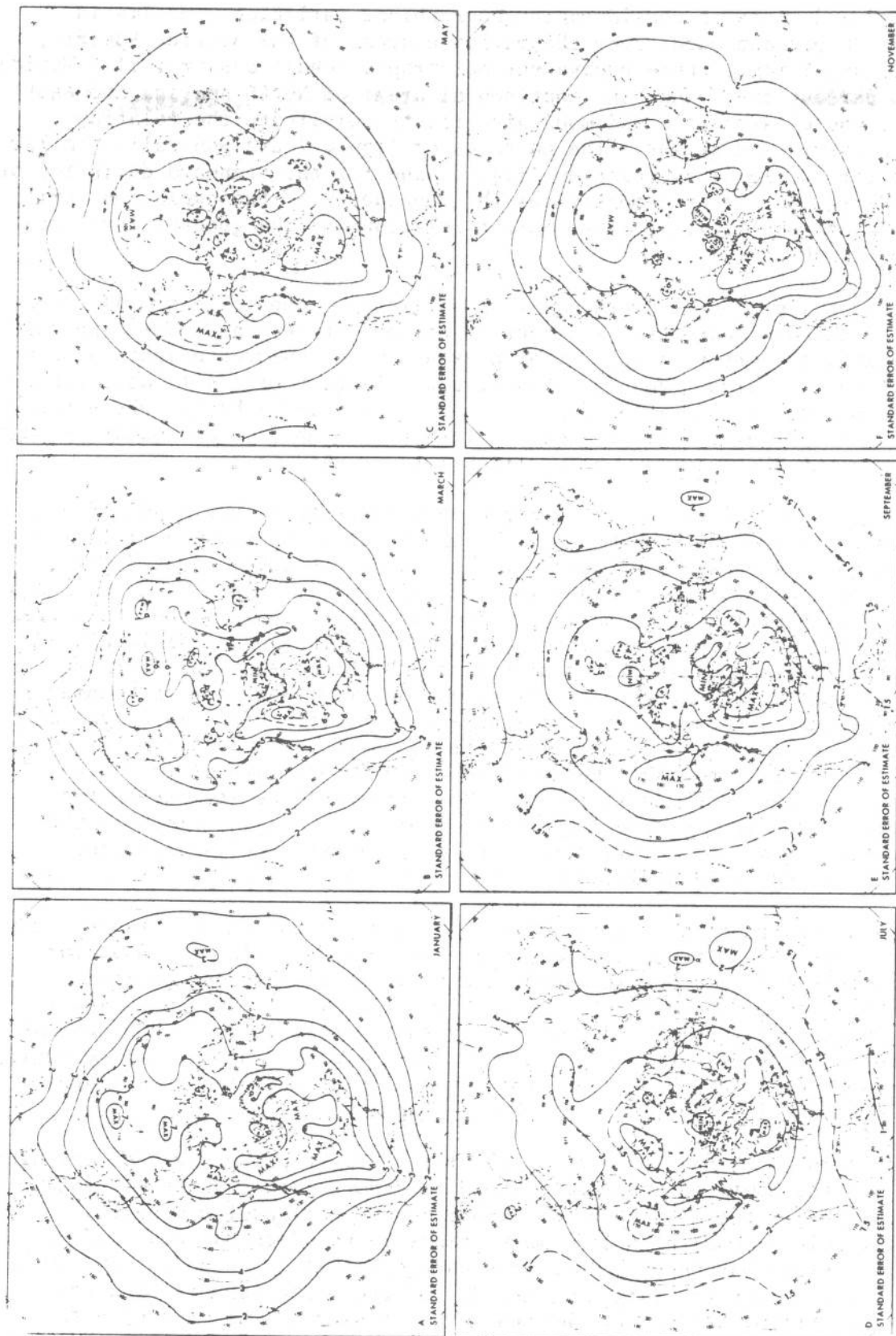


Figure 8. - Standard error of estimate (mb.) in specifying sea level pressure from concurrent 700-mb. heights for months shown, with centers labeled as maximum or minimum.

in summer, and there is considerable geographical variation. Maxima in excess of 80 percent occur over the maritime areas of the Arctic, Pacific, Atlantic, and Europe, where equivalent barotropic conditions prevail. Minima under 60 percent are found over continental areas of North America and eastern Asia, where baroclinic and mountain effects complicate the relation between pressure and height. The patterns of figure 7 are generally similar to those for the local correlation (fig. 4) and for the standard deviation of pressure (fig. 3). This demonstrates the dependence of the explained variance upon both the local pressure-height relation and the general level of pressure variability.

Figure 8 maps the standard error of estimate of predictions made from the specification equations. In about 68 percent of the cases for a normal distribution, the error in specifying pressure from observed heights should be less than the values shown in this figure. Largest errors (7 mb.) can be expected in January and March in portions of Canada and Siberia, where the specification is poor; smallest errors (less than 2 mb.) should occur throughout the year in the Tropics, where variability is very low.

Figure 9 summarizes values averaged on a hemispheric basis as a function of latitude for the month of March. The upper curves show the correlation coefficients between sea level pressure and 700-mb. height, plotted first for strictly local values and then for the multiple correlation coefficients of the final specification equations. The difference between the two curves represents the improvement obtained by considering the entire field of 700-mb. height instead of just the local height. Both correlations diminish sharply at low latitudes, where analysis and observational errors become of great importance because of small pressure variability. This is illustrated by the lower curves, which give, first the standard deviation of observed sea level pressure, and then the standard error of estimate of the specification equations, both in millibars. The difference between these two curves gives some idea of the improvement over climatology yielded by the specification equations. This difference is greatest at high latitudes, where both the standard deviation and the multiple correlation are largest.

Similar information on latitudinal averages is contained in table 2 for all months studied. The distributions are generally similar to those for March plotted in figure 9. The explained variance reaches one maximum around 60°N. and another at 80°N. during practically all months. However, values are generally somewhat lower during summer than in the other seasons. The standard error of estimate has a less regular distribution, but generally peaks between 65°N. and 75°N. For the hemisphere as a whole, it averages about 2 mb. less in July (2.8 mb.) than in January (4.9 mb.).

Figure 10 shows the location of the first height picked by the screening program for the month of November. The dots denote points where the local 700-mb. height is the most important predictor of sea level pressure. Nearly all points in both oceans, many points in northern Eurasia, and many points in eastern Canada fall into this category. At a few points in southern Asia, denoted by the letter D, the day of the month is more important than any height in determining the sea level pressure. This reflects the well known monsoonal increase of sea level pressure during the fall. In the remainder of the hemisphere the first 700-mb. height selected is located west

or north of the reference point. The location of the height is given by the tail of the arrows in figure 10, the reference point by the head.

Selection of the final multiple regression equations was made using the customary 2 percent cutoff criterion [5], except that the local height and the day of the month were selected as long as they contributed as little as 1 percent toward explaining the pressure variance. Even so, it was rarely necessary to use more than six variables, and the average number was three or four. The exact number used in November is mapped in figure 11, where the stippled area denotes one or two variables in the equation (Atlantic, Pacific, and Arctic Oceans), and the hatched area denotes five or six variables (continental areas).

Figure 12 delineates a few areas of the hemisphere which do not select the local 700-mb. height as one of the variables in the final specification equations for November. They occur mostly in the Arctic and Eastern Hemisphere. The bulk of the map is blank, denoting that the local height is picked as one of the predictors.

Figure 13 is similar to figure 12, but for the day of the month. The areas hatched are those where the day does not appear in the final equation, mostly over oceans. In the blank areas the day is selected as one of the variables, although usually contributing only a few percent to the explained variance. Thus these are areas where the seasonal trend is of some importance, but it is dominant only in the monsoonal areas of southern Asia marked by D in figure 10.

Charts like figures 10-13 were prepared for the other months of the year, but are not reproduced here. Instead, some of their properties are summarized in the last three columns of table 2, which gives latitudinal averages by month. The number of variables in the regression equations is generally greater at low than at high latitudes, with more in fall and spring than in winter or summer. The percent of points for which the local height is selected is also greater at low than at high latitudes, with smaller values in spring than at any other time of year. The percent of points for which the day of the year is selected shows the expected seasonal trend, with maxima in May

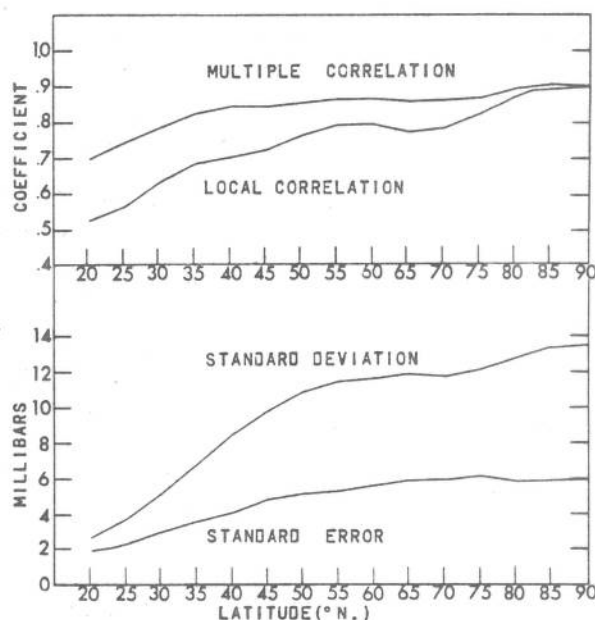


Figure 9. - Values during March averaged over the Northern Hemisphere as a function of latitude for: (a) the multiple correlation between observed pressures and those given by the specification equations, (b) the local correlation between pressure and height at the same point, (c) the standard deviation of observed pressure, and (d) the standard error of estimate for pressures forecast from the specification equation.

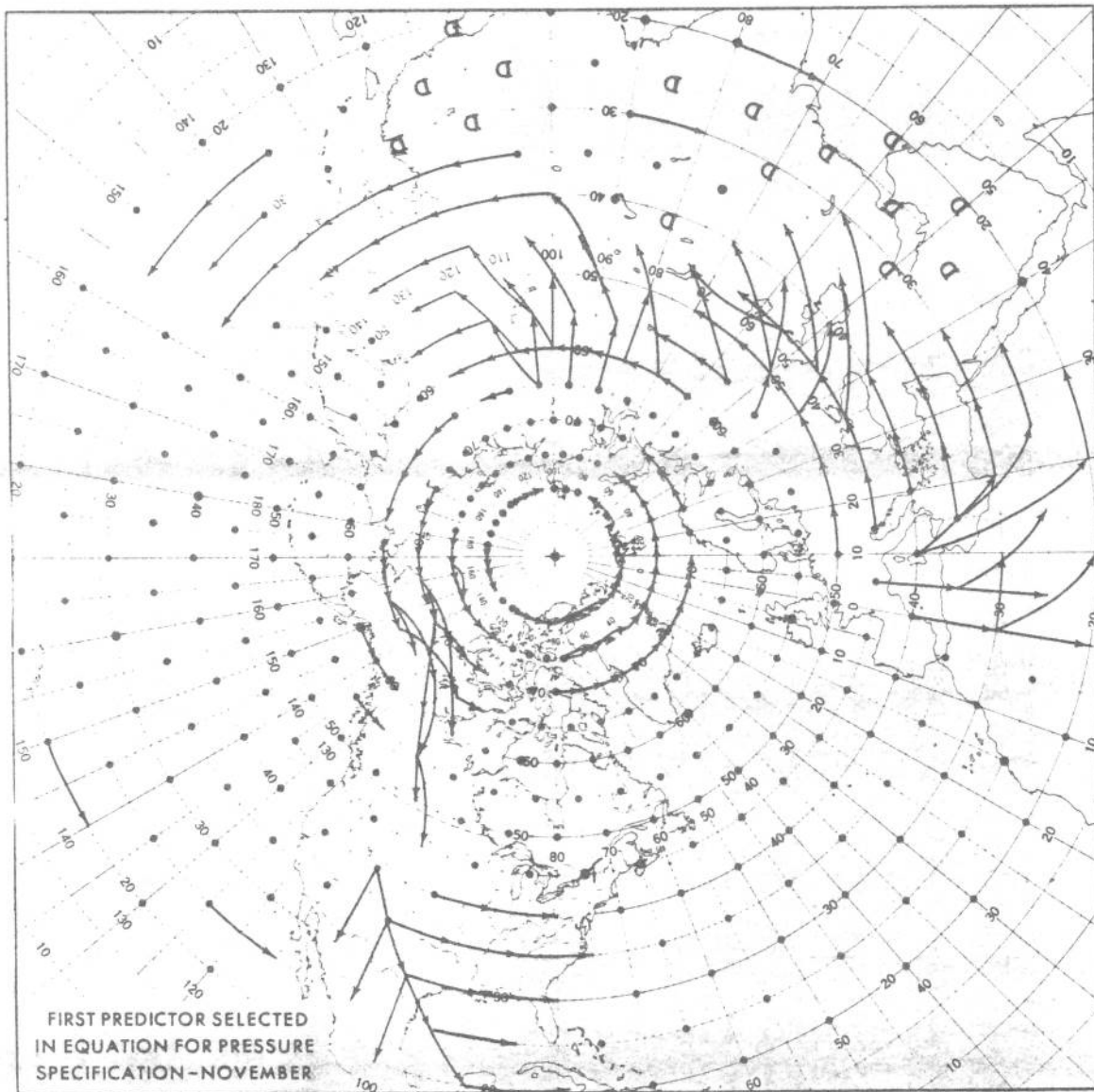


Figure 10. - Location of the first variable selected by the screening program in the equations for specifying sea level pressure in November from concurrent 700-mb. height. The local height was picked at points shown by dots, the day of the month at points marked D, and the upstream height at points with arrows which originate at the predictor height and terminate at the predictand pressure.

and September and minima in January and July. For the mean of all latitudes and months, the equations explain 68 percent of the pressure variance by means of three variables, have a standard error of almost 4 mb., contain the local height at 70 percent of the points, and select the day of the year 45 percent of the time.

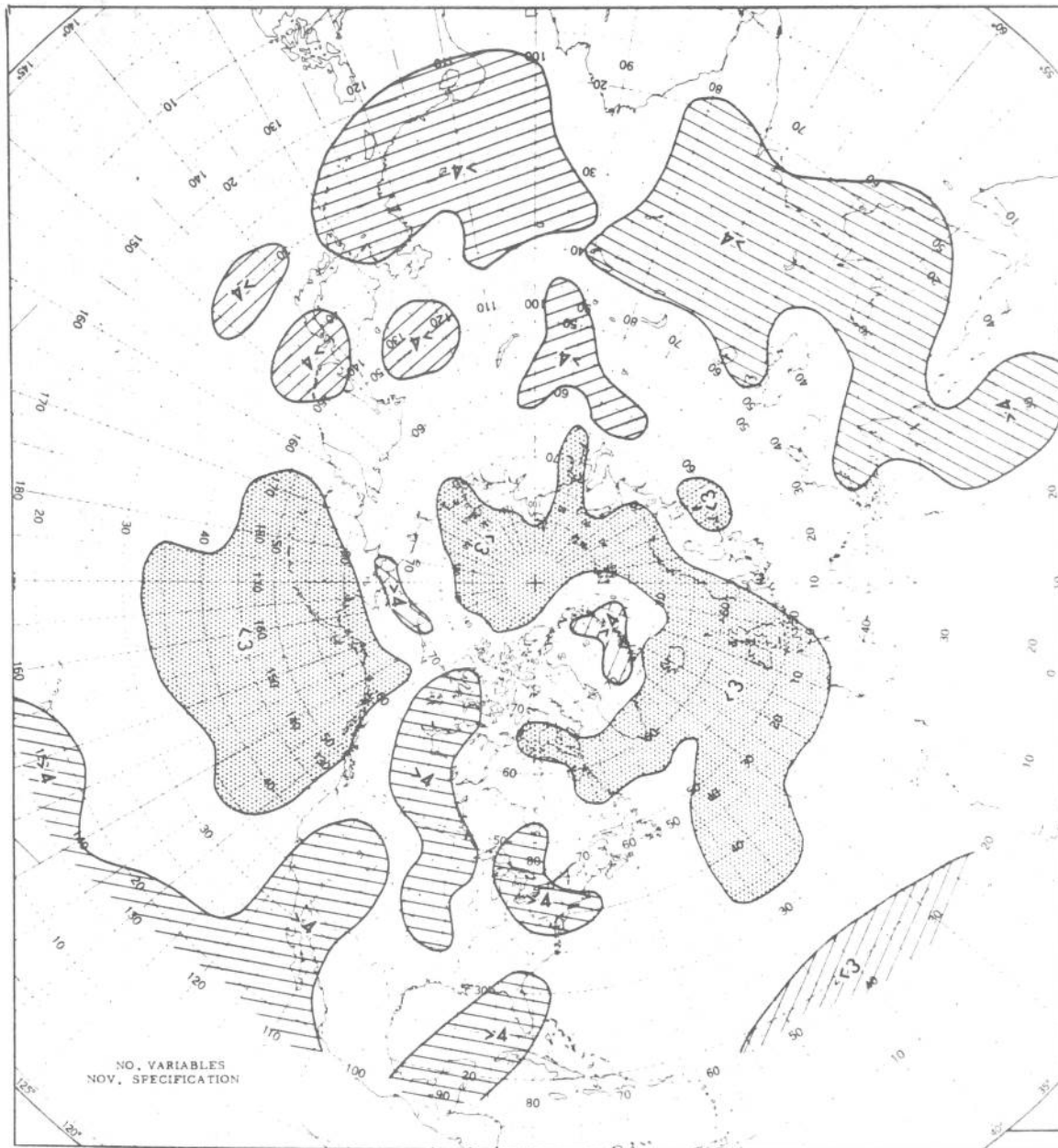


Figure 11. - Number of variables in equations for specifying sea level pressure in November from concurrent 700-mb. height. Areas with more than four variables are hatched, less than three variables stippled, and three or four variables blank.

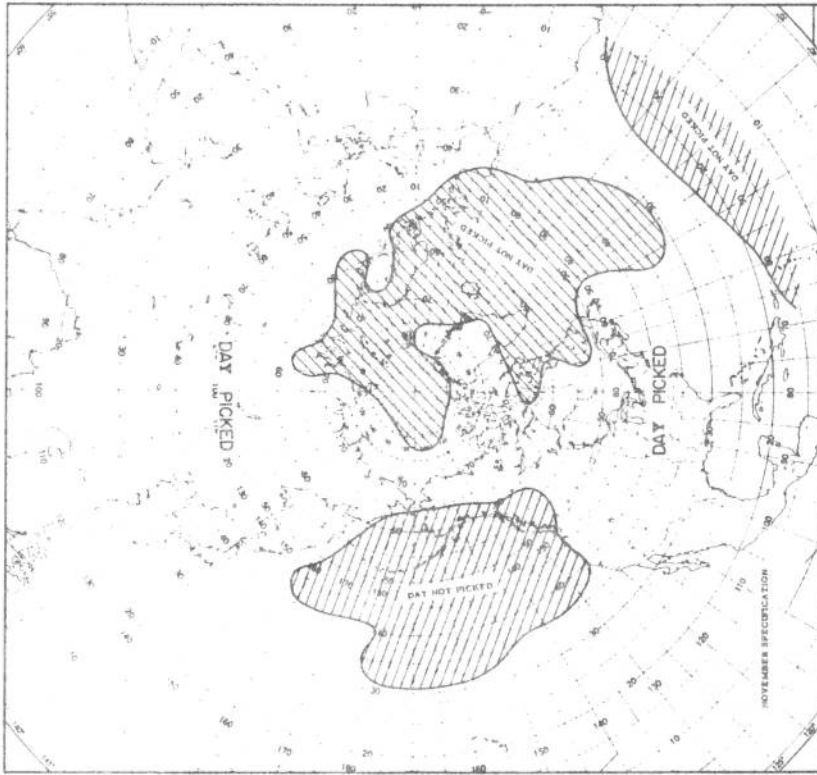


Figure 13. - Areas in which the day of the month was selected (unshaded) and not selected (hatched) as a predictor in the equations for specifying sea level pressure in November from concurrent 700-mb. height.

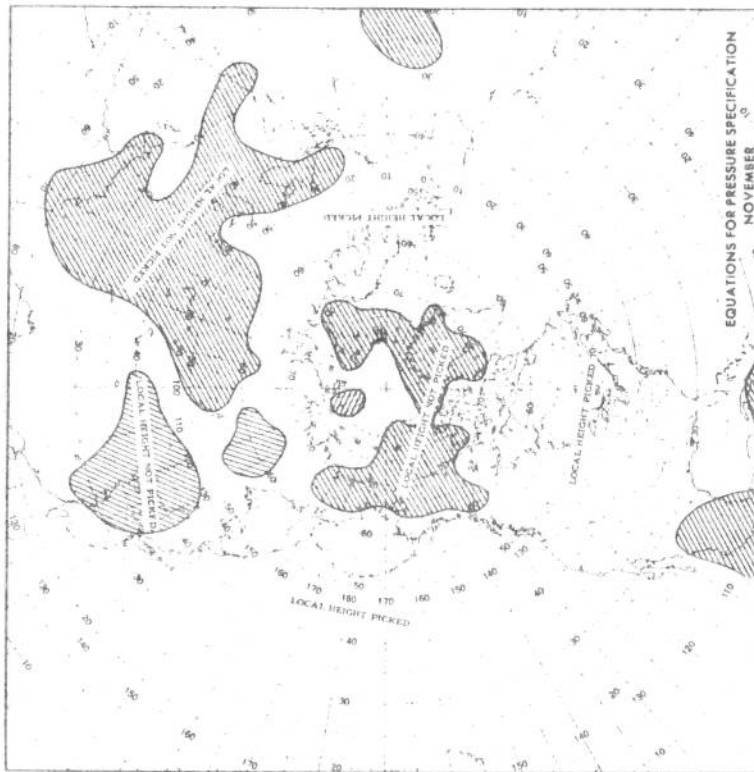


Figure 12. - Areas in which the local height was selected (unshaded) and not selected (hatched) as a predictor in the equations for specifying sea level pressure in November from concurrent 700-mb. height.

5. OPERATIONAL ASPECTS

In order to apply the daily specification equations on a routine basis, a program was written for the IBM 7094 which solves the multiple regression equations at each of 469 latitude-longitude grid points, interpolates by spatial harmonic analysis to give predicted pressures at each of 1977 points of the square grid used in numerical weather prediction [3], and then makes use of the electronic curve-follower to draw isobars. At 10°N . and 15°N ., where no derivations were made because of inadequate data, the specification equations of 20°N . or 25°N . are assumed to apply unchanged at each longitude except for a 10° southward shift of all points in the equation. At 85°N ., where no grid point data are available, predicted pressures are obtained by interpolation between computed values at 80°N . and the North Pole.

By means of this program, a completely mechanical map of the sea level pressure distribution over the entire Northern Hemisphere north of 10°N . can be obtained in a few minutes from any 700-mb. map. Beginning in November 1963, this program has been applied to numerical height forecasts for 36 or 72 hr. in advance and used experimentally in the National Meteorological Center. Since the equations are available only for every other month of the year, each set is used for a 2-month period extending from mid-month of the month preceding derivation to mid-month of the following month. For example, the equations for July are applied from June 15 through August 14, the equations for September from August 15 through October 14, etc.

A sample objective forecast for 36 hr. in advance is illustrated in figure 14. This prediction was made by applying the November specification equations to the baroclinic prognostic heights at 700 mb. made at 1200 GMT, November 16, 1963, and valid at 0000 GMT, November 18. Comparison with the verifying map observed on November 18 (fig. 15) reveals that the objective forecast is quite good in large-scale pattern but deficient in important detail. For example, deep Lows are missed in the eastern Pacific, Hudson Bay, northern Russia, and eastern Siberia. The objective map is also lacking in character at low latitudes, where a closed Low west of the Hawaiian Islands is not caught. On the other hand, Highs over Bermuda, Alaska, Gibraltar, and Siberia, and Lows over the Atlantic, Kamchatka, and British Columbia, are all handled well.

It is apparent from these figures, as well as from routine inspection of the daily maps, that the objective forecasts tend toward excessive smoothness of pattern and tend to eliminate small-scale details which are frequently observed on actual sea level pressure charts. In this respect the objectives look more like space- or time-means than like forecasts prepared by conventional or dynamical methods. For this reason they have been found quite useful in preparing 5-day and 30-day mean predictions and are applied routinely for this purpose in the Extended Forecast Division of NMC. However, they are considered too smooth for daily forecasting.

One reason for this condition is the nature of the numerical height forecasts. Because they are systematically filtered every 12 hr. to minimize noise and truncation errors, the prognostic upper-air chart is smoother and has less variability than its corresponding observed chart. This is illustrated

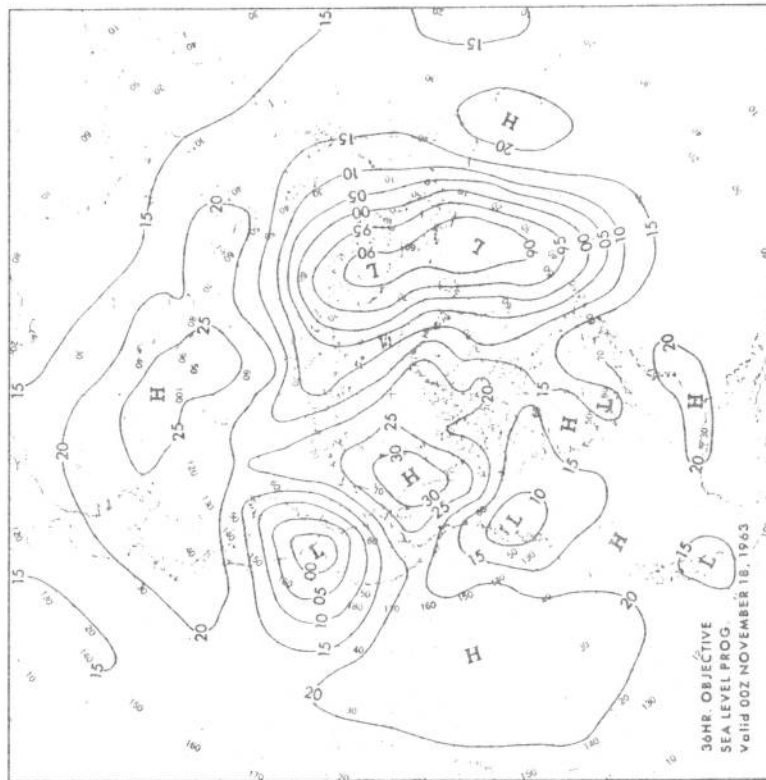


Figure 14. - Objective forecast of sea level pressure made by applying the November specification equations to the 36-hr. baroclinic prognostic 700-mb. heights valid at 0000 GMT, November 18, 1963. Isobars are drawn for every 5 mb. and labeled with last two digits only.

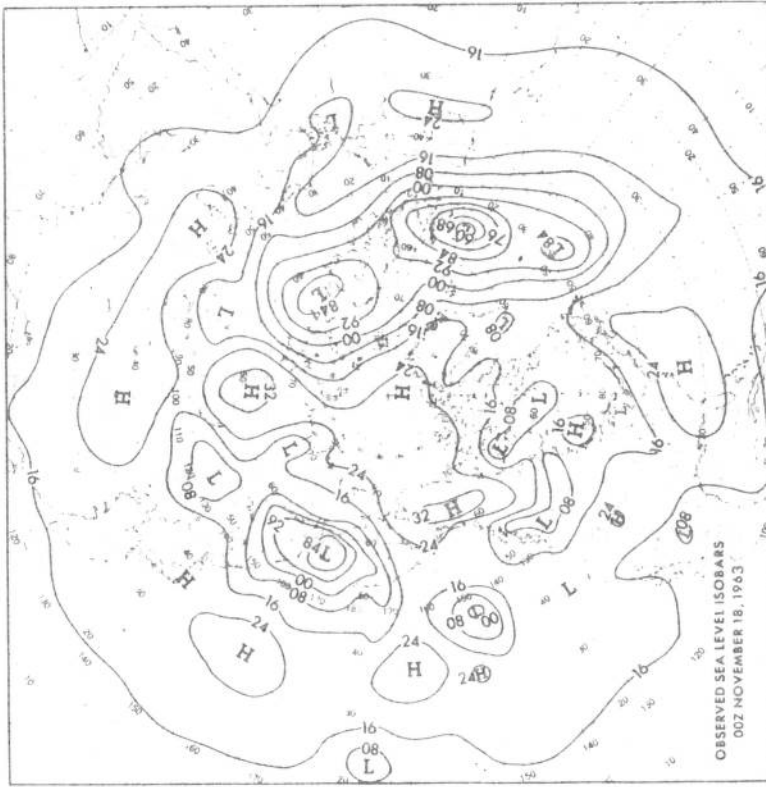


Figure 15. - Sea level pressure observed at 0000 GMT, November 18, 1963. Isobars are drawn for every 8 mb. and labeled with last two digits only.

by figure 16, which gives the geographical distribution of the ratio of the observed standard deviation of 700-mb. height anomaly to that forecast by 36-hr. baroclinic prognoses prepared routinely in the National Meteorological Center by the 3-level model of Cressman [2]. This ratio was computed separately at each grid point by combining 9 months of the cool season from November 1962 through January 1964. The ratio is less than 1 in a few areas (shaded) where the forecasts call for too much variability. However, in most of the hemisphere, especially at middle latitudes, ratios greater than 1 show that the numerical model is underforecasting. This tendency is most marked in the central Pacific, where only 2/3 of the observed variability is being forecast.

The numerical prognoses are subject to another type of systematic error because of their bias. This is illustrated by figure 17, which maps the average difference between 36-hr. forecast and observed 700-mb. heights for the same 9 months used previously. Negative values in the shaded areas denote that prognostic heights average lower than observed. Positive values reach maxima of 180 ft. in the central Pacific and 160 ft. off Newfoundland. Here neglect of diabatic heating and subsequent cyclogenesis may cause forecast heights to average too high. This figure suggests other systematic errors of the numerical forecasts such as excessive northward transport of momentum, retrogression of the ultralong waves, spurious anticyclogenesis of the subtropical Highs, and complex mountain effects.

Figure 18 illustrates the procedure that was followed in order to attempt to overcome these difficulties. The first equation shows that the heights forecast by the numerical model were corrected for their bias, expressed in anomaly form by subtracting the normal height, "desmoothed" by multiplying by the ratio of observed to standard deviation, and finally added again to the normal.

The heights corrected in this way were substituted into the multiple regression equations to yield regression pressures (p_r). These were too weak in intensity of pressure centers because regression forecasts always tend to return toward the mean. This difficulty was partly overcome, as shown in the second equation, by subtracting the normal pressure from the regression pressure, dividing by the multiple correlation coefficient, and adding the inflated anomaly to the normal. Sea level pressures forecast by means of these two equations should have about the same variability as those observed [8, 5].

6. VERIFICATION AND CONCLUSION

Objective pressure forecasts were made by this method from the NMC 36-hr. baroclinic 700-mb. prognoses twice each day during an independent test period of February and March 1964. Figure 19 gives a sample forecast (left) along with its verifying map (right). The forecasts were verified by means of the S-1 score, a measure of relative pressure gradient error which varies from 0 for a perfect prediction through 100 for no skill, to 200 for the worst possible forecast [23]. The score for this particular map over the North American area was 65, but the average score for all 62 forecasts in the sample was 75, as shown in table 3. This was superior to the average score of 91 made by persistence, about equal to the score of 75 obtained for sea level forecasts made by the Reed [16] dynamic model for the same sample, and inferior to the average

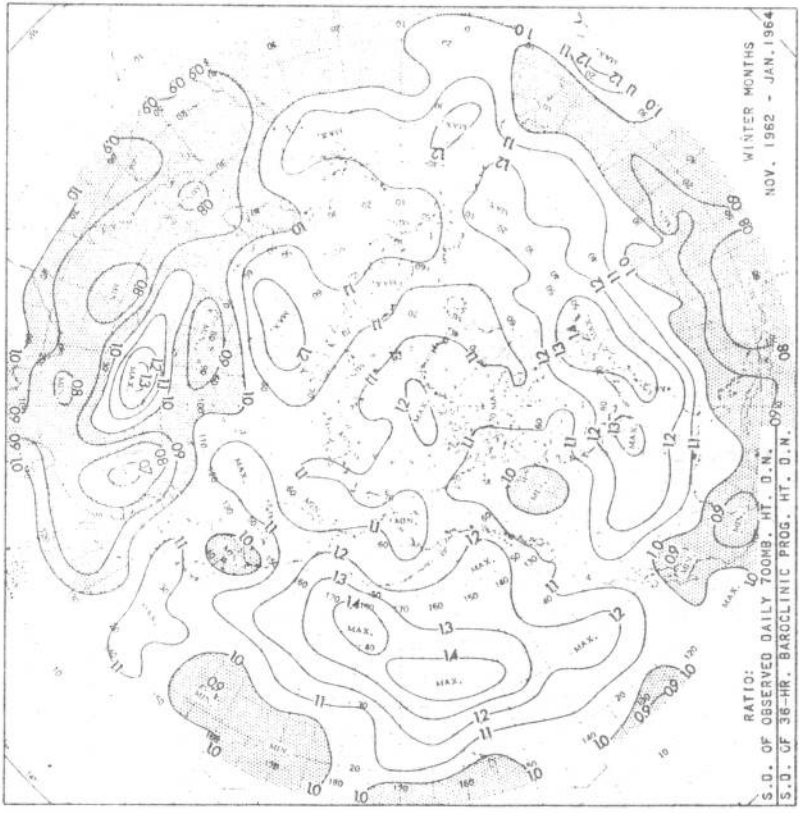


Figure 16. - Geographical distribution of the ratio: standard deviation of observed daily 700-mb. height anomaly to standard deviation of 36-hr. baroclinic prognostic height anomaly, computed for 9 months of the cool season (Nov.-Apr.) from November 1962 through January 1964. Ratios less than 1 are shaded, and centers are labeled as maximum or minimum.

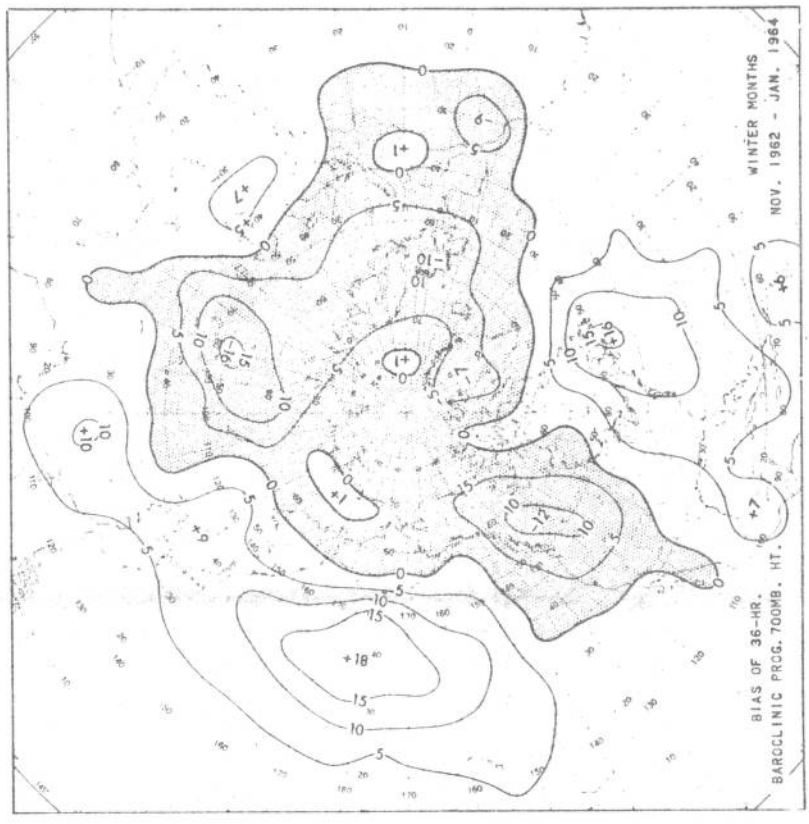


Figure 17. - Average values of the difference: 36-hr. baroclinic prognostic 700-mb. height minus verifying observed height, computed for 9 months of the cool season from November 1962 through January 1964. Isopleths and centers are labeled in tens of feet with negative values shaded.

1. To correct numerical heights:

$$H_c = \frac{S_o}{S_f} (H_f - B - H_n) + H_n$$

where: H_c is corrected height

S_o is standard deviation of observed height

S_f is standard deviation of forecast height

H_f is height forecast by numerical model

B is bias of numerical prognostic height = $\overline{H_f} - \overline{H_o}$

H_n is normal height

2. To inflate regression pressures:

$$P_f = \frac{1}{R} (P_r - P_n) + P_n$$

where: P_f is forecast pressure

R is multiple correlation coefficient

P_r is pressure computed from multiple regression equation

P_n is normal pressure

Figure 18. - Equations used to: (1) correct numerical prognostic heights for bias and insufficient variability, and (2) increase variability of pressures forecast from regression equations.

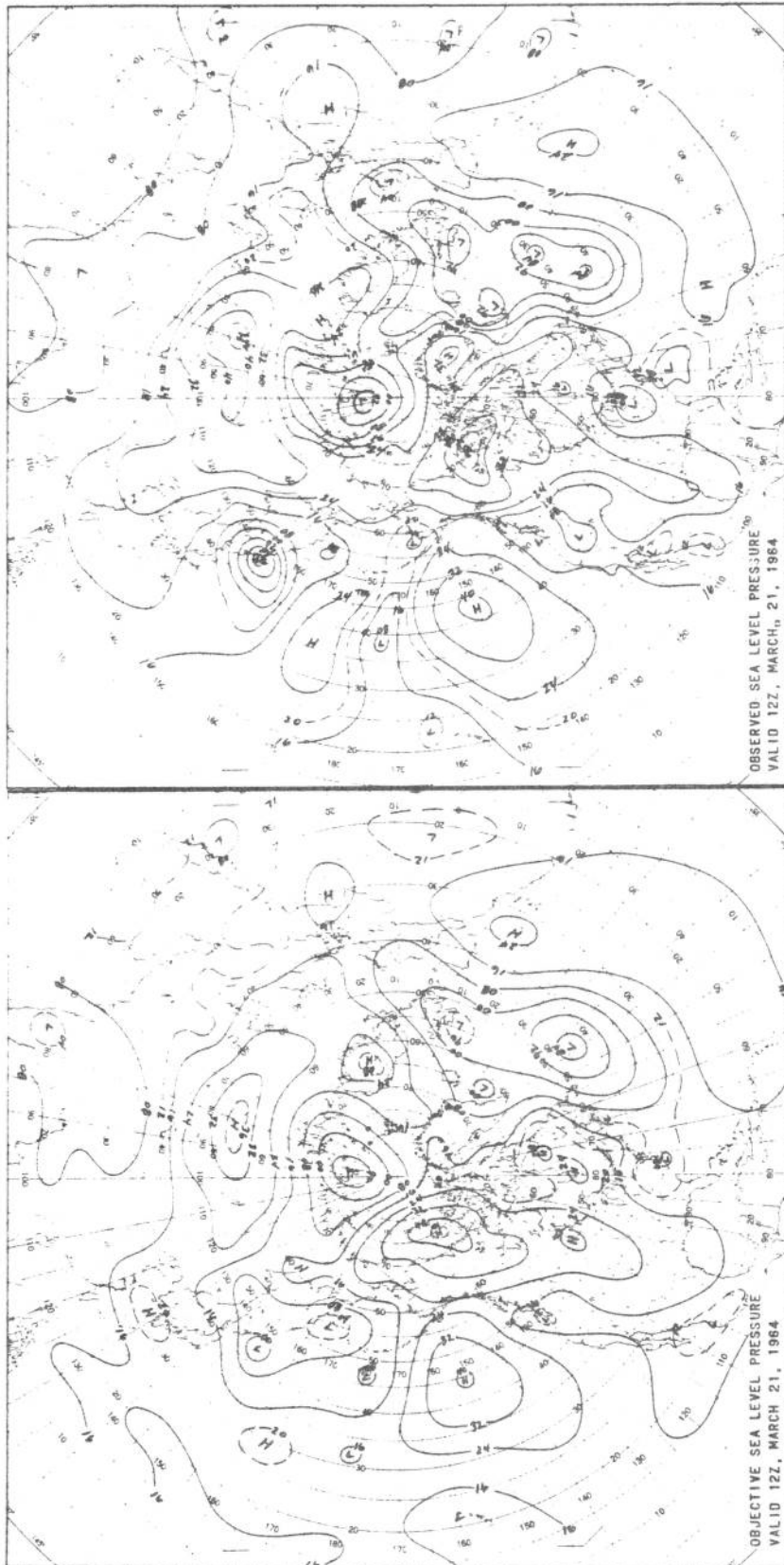


Figure 19. - Objective forecast of sea level pressure made by applying the March specification equations and the corrections of figure 18 to the 36-hr. baroclinic prognostic 700-mb. heights valid at 1200 GMT, March 21, 1964, with verifying map on the right. Isobars are drawn for every 8 mb., with intermediate lines dashed and labeled with last two digits only.

Table 3. - Verification of twice-daily sea level pressure forecasts over North America for 62 cases for March 1964 in terms of the S-1 score and the average absolute error. (In each case, the lower the score, the better.)

<u>Type of Forecast</u>	<u>Period</u>	<u>S-1 Score</u>	<u>Error (mb.)</u>
Objective (specification)	36-hr.	75.3	6.1
Persistence (last observed)	36-hr.	91.0	8.6
Reed model (dynamic)	36-hr.	74.1	7.1
Conventional (NMC)	30-hr.	63.3	5.2

score of 63 yielded by the 30-hr. prognoses prepared subjectively by experienced forecasters of NMC. It should be remembered, however, that the forecasters had the benefit of 6 hr. later sea level data, as well as the Reed 36-hr. 1000-mb. prognoses as forecast aids.

The average pressure error in millibars was also computed for each forecast, with scores summarized on the right side of table 3. The relative rank in terms of this statistic was generally similar to that obtained with the S-1 score, except for an interchange of order between the objective specifications and the Reed dynamic model.

The specification equations were also applied experimentally to the primitive equation model of Shuman [22]. Here no corrections of the type illustrated in figures 16 and 17 were made because this model appears to exhibit greater variability and less bias than the filtered baroclinic model. An example of an objective sea level pressure map for 36 hr. in advance specified from prognostic 700-mb. heights produced by the primitive equation model is shown in figure 20 for December 9, 1963. Comparison with the verifying (observed) map on the right shows that the principal features are well depicted, but again with insufficient small-scale detail.

In order to determine whether the lack of detail in the objective specifications is inherent in the regression equations, they were applied to the 700-mb. map actually observed at 1200 GMT, January 7, 1966, thereby assuming that a perfect upper-air prognosis was available for that date. The resulting specification is shown in figure 21, and the corresponding observed sea level pressure map is given in figure 22. Once again there is insufficient detail in the specified map, but the discrepancy is not as great as it was in the case in which prognostic heights were used (figs. 14, 19, and 20). However, the central intensity of pressure systems appears to be generally underforecast in the specified map. Although the principal circulation features are generally well depicted, the specification is considerably poorer in North America than

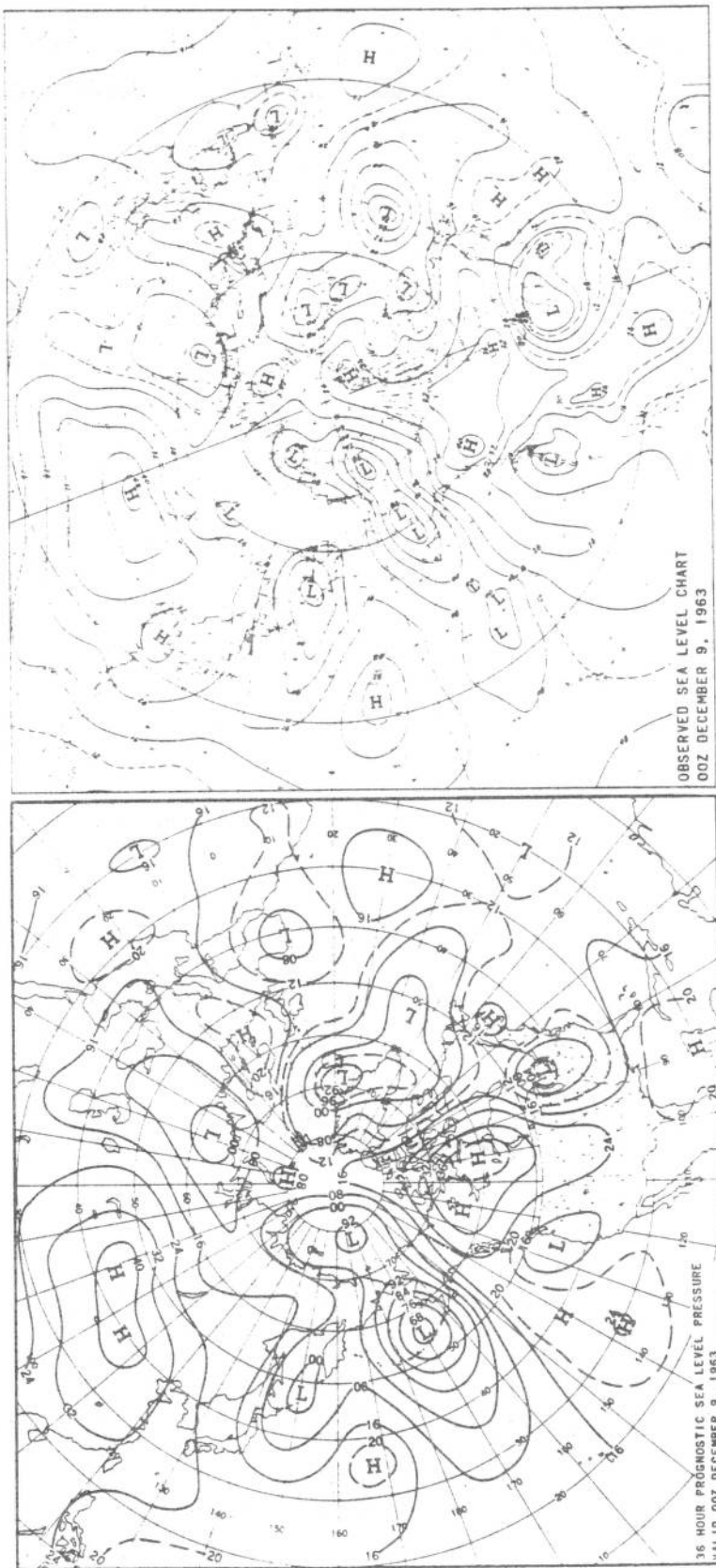


Figure 20. - Objective forecast of sea level pressure made by applying the November specifications equations to the 36-hr. prognostic 700-mb. heights produced by the primitive equation model. The forecast, valid at 0000 GMT on December 9, 1963, is on the left, and the verifying map is on the right. Isobars are drawn for every 8 mb., with intermediate lines dashed, and labeled with last two digits only.

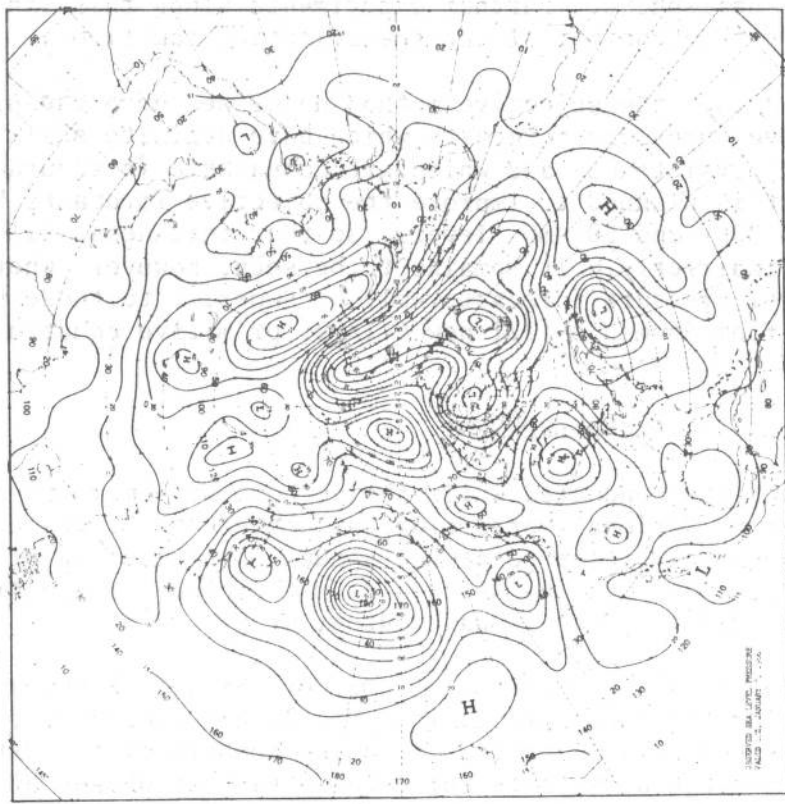


Figure 21. - Objective specification of sea level pressure made by applying the January specification equations to the 700-mb. heights observed at 1200 GMT, January 7, 1966. Isobars are drawn for every 4 mb. and labeled with last two digits only.

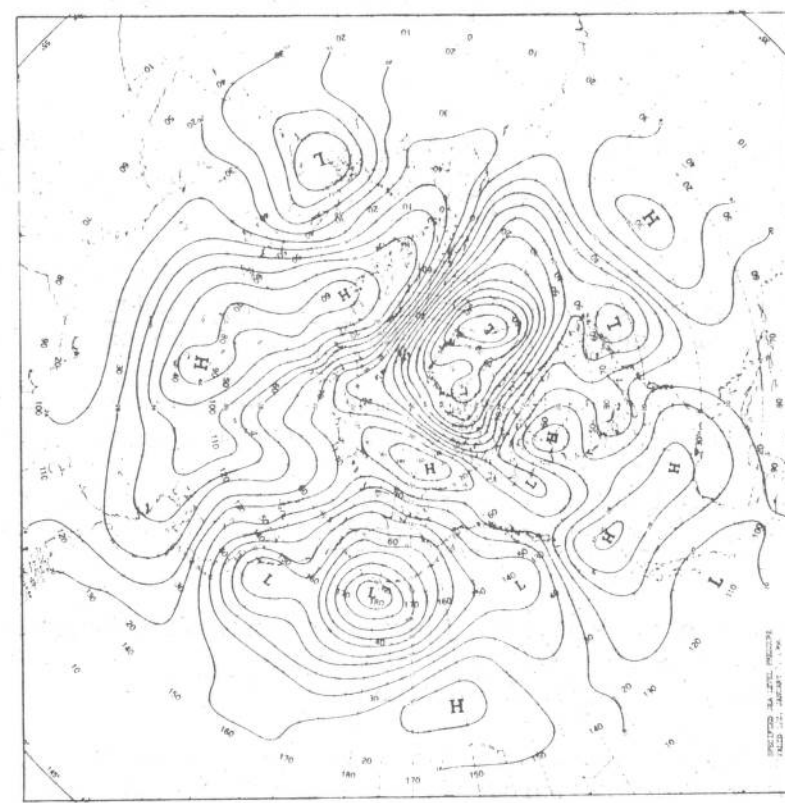


Figure 22. - Sea level pressure observed at 1200 GMT, January 7, 1966. Isobars are drawn for every 5 mb. and labeled with last two digits only.

in the remainder of the hemisphere. Further experiments along this line may shed additional light on the behavior of the specification equations.

It may be concluded that the objective method described here can produce in a few minutes sea level pressure forecasts which have definite skill beyond chance, climatology, or persistence, and which are comparable in accuracy to dynamical forecasts. It is planned to improve the objective forecasts by incorporating data from 850- and 500-mb. levels, so that thickness will enter explicitly rather than indirectly. It remains to be seen, however, whether these objective sea level pressure forecasts will be superior to those produced directly (dynamically) from Shuman's [22] new 6-layer primitive equations model.

ACKNOWLEDGMENT

Most of this project was conducted while the authors were members of the Extended Forecast Division, National Meteorological Center, U. S. Weather Bureau. Part of the paper was presented at the annual joint meeting of the American Meteorological Society and the Section of Meteorology of the American Geophysical Union, April 21-24, 1964, in Washington, D. C.

The authors wish to thank the Director of NMC, Dr. Frederick Shuman, and the Associate Director for Extended Forecasting, Mr. Jerome Namias, for permission to conduct the study, as well as the following members of the Extended Forecast Division for valuable assistance received in various phases of the data processing: James F. Andrews, Robert H. Gelhard, Curtis W. Crockett, Donovan J. Truesdell, Thomas H. Johnson, and Miss Myrtle M. Wagner.

REFERENCES

1. H. Arakawa, "Statistical Method to Forecast the Movement and the Central Pressure of Typhoons in the Western North Pacific," Journal of Applied Meteorology, vol. 3, No. 5, Oct. 1964, pp. 524-528.
2. G. P. Cressman, "A Three-Level Model Suitable for Daily Numerical Forecasting," National Meteorological Center Technical Memorandum No. 22, U. S. Weather Bureau, Washington, D. C., 1963, 27 pp. + 15 pp. of figures.
3. E. B. Fawcett, "Six Years of Operational Numerical Weather Prediction," Journal of Applied Meteorology, vol. 1, No. 3, Sept. 1962, pp. 318-332.
4. D. G. Friedman, "Specification of Temperature and Precipitation in Terms of Circulation Patterns," Journal of Meteorology, vol. 12, No. 5, Oct. 1955, pp. 428-435.
5. W. H. Klein, "Application of Synoptic Climatology and Short-Range Numerical Prediction to Five-Day Forecasting," Research Paper No. 46, U. S. Weather Bureau, Washington, D. C., June 1965, 109 pp.
6. W. H. Klein, "A Hemispheric Study of Daily Pressure Variability at Sea Level and Aloft," Journal of Meteorology, vol. 8, No. 5, Oct. 1951, pp. 332-346.

7. W. H. Klein, C. W. Crockett, and J. F. Andrews, "Objective Prediction of Daily Precipitation and Cloudiness," Journal of Geophysical Research, vol. 70, No. 4, Feb. 15, 1965, pp. 801-813.
8. W. H. Klein, B. M. Lewis, C. W. Crockett, and I. Enger, "Application of Numerical Prognostic Heights to Surface Temperature Forecasts," Tellus, vol. 12, No. 4, Nov. 1960, pp. 378-392.
9. B. M. Lewis, "Normal 700-mb. Height and Sea Level Pressure Obtained by Harmonic Smoothing of Observed Data," Extended Forecast Division, Unpublished manuscript, Aug. 1964, 5 pp.
10. E. N. Lorenz, "Empirical Orthogonal Functions and Statistical Weather Prediction," Statistical Forecasting Project, Scientific Report No. 1, Contract No. AF19(604)-1566, Department of Meteorology, Massachusetts Institute of Technology, Cambridge, Mass., Dec. 1956, 49 pp.
11. I. A. Lund, "Experiments in Predicting Sea-Level Pressure Changes for Periods of Less Than Twelve Hours," Journal of Applied Meteorology, vol. 2, No. 4, Aug. 1963, pp. 517-525.
12. F. L. Martin, J. R. Borsting, F. J. Steckbeck, and A. H. Manhard, Jr., "Statistical Prediction Methods for North American Anticyclones," Journal of Applied Meteorology, vol. 2, No. 4, Aug. 1963, pp. 508-516.
13. R. G. Miller, "The Screening Procedure. A Statistical Procedure for Screening Predictors in Multiple Regression. Part II," Studies in Statistical Weather Prediction, Final Report, Contract No. AF19(604)-1590, Travelers Weather Research Center, Hartford, Conn., edited by B. Shorr, Dec. 31, 1958, pp. 86-136.
14. R. G. Miller and T. F. Malone, "The Application of Synoptic Climatology to the Prediction of Sea-Level Circulation Patterns, Part III-F," Studies in Synoptic Climatology, Final Report on Synoptic Climatology Project No. N50ri-07883, Department of Meteorology, Massachusetts Institute of Technology, Cambridge, Mass., edited by W. D. Sellers, March 15, 1956, pp. 115-122.
15. B. Ratner, "Upper-Air Climatology of the United States, Part 2 - Extremes and Standard Deviations of Average Heights and Temperature," U. S. Weather Bureau Technical Paper No. 32, Washington, D. C. 1958, 140 pp.
16. R. J. Reed, "Experiments in 1000-mb. Prognosis," National Meteorological Center Technical Memorandum No. 26, U. S. Weather Bureau, Washington, D. C., 1963, 31 pp. + 11 pp. of figures.
17. J. A. Russo, Jr. and R. G. Harris, "Statistical Specification and Prediction of Sea-Level Pressure from 700- and 500-mb. Heights," Paper presented at 237th National Meeting of the American Meteorological Society, April 19-22, 1965, Washington, D. C. (Abstract in Bulletin of the American Meteorological Society, vol. 46, No. 2, Feb. 1965, p. 75.)

18. J. A. Russo, Jr., I. Enger, and E. L. Sorenson, "A Statistical Approach to the Short-Period Prediction of Surface Winds," Journal of Applied Meteorology, vol. 3, No. 2, Apr. 1964, pp. 126-131.
19. T. E. W. Schumann, "An Enquiry into the Possibilities and Limits of Statistical Weather Forecasting," Quarterly Journal of the Royal Meteorological Society, vol. 70, No. 305, July 1944, pp. 181-195.
20. T. E. W. Schumann and M. P. Van Rooy, "Analysis of the Standard Deviation of Atmospheric Pressure over the Northern Hemisphere," Department of Transport, Weather Bureau, W. B. 16, Pretoria, South Africa, 1951, 21 pp.
21. B. Shorr, "Empirical Orthogonal Functions Applied to Prediction of the Sea-Level Pressure Field," Statistical Forecasting Project, Scientific Report No. 3, Contract No. AF19(604)-1566, Department of Meteorology, Massachusetts Institute of Technology, Cambridge, Mass., Nov. 1957, 88 pp.
22. F. G. Shuman, "A Multi-Level Primitive Equation Model," unpublished manuscript, National Meteorological Center, U. S. Weather Bureau, Nov. 1965, 21 pp.
23. S. Teweles, Jr., and H. B. Wobus, "Verification of Prognostic Charts," Bulletin of the American Meteorological Society, vol. 35, No. 10, Dec. 1954, pp. 455-463.
24. K. W. Veigas, R. G. Miller, and C. M. Howe, "Probabilistic Prediction of Hurricane Movements by Synoptic Climatology, Part III-B," Studies in Statistical Weather Prediction, Final Report, Contract No. AF19(604)-1590, Travelers Weather Research Center, Hartford, Conn., edited by B. Shorr, Dec. 31, 1958, pp. 154-202.
25. K. W. Veigas and F. P. Ostby, Jr., "Application of a Moving-Coordinate Prediction Model to East Coast Cyclones," Journal of Applied Meteorology, vol. 2, No. 1, Feb. 1963, pp. 24-38.
26. G. P. Wadsworth, "Short Range and Extended Forecasting by Statistical Methods," Air Weather Service Technical Report No. 105-38, U. S. Air Force, Headquarters, Air Weather Service, Washington, D. C., Feb. 1948, 202 pp.
27. R. M. White, D. S. Cooley, R. C. Derby, and F. A. Seaver, "The Development of Efficient Linear Statistical Operators for the Prediction of Sea-Level Pressure," Journal of Meteorology, vol. 15, No. 5, Oct. 1958, pp. 426-434.

